UWB SHARE-APERTURE ANTENNA FOR 5G SUB-6G APPLICATIONS

A PROJECT REPORT

SUBMITTED IN PARTIAL FULFILLMENT OF THE REQUIREMENTS FOR THE AWARD OF THE DEGREE OF

BACHELOR OF TECHNOLOGY

IN

ELECTRONICS AND COMMUNICATION ENGINEERING

Submitted by:

PIYUSH KUMAR SINGH (2K20/EC/144)

ROHIT SINGH (2K20/EC/171)

RUDRA (2K20/EC/172)

Under the supervision of

DR. PRIYANKA JAIN

(Professor)

ELECTRONIC AND COMMUNICATION ENGINEERING

DELHI TECHNOLOGICAL UNIVERSITY

(Formerly Delhi College of Engineering)

Bawana Road, Delhi-110042

MAY,2024

DELHI TECHNOLOGICAL UNIVERSITY

(Formerly Delhi College of Engineering)

Bawana Road, Delhi-110042

CANDIDATES'S DECLARATION

We, Piyush Kumar Singh (2K20/EC/144), Rohit Singh (2K20/EC/171), Rudra (2K20/EC/172) students of B.Tech. Department of Electronic and Communication Engineering, hereby declare that project Dissertation titled "**UWB Share-Aperture Antenna for 5G Sub-6G Applications**" which is submitted by us to the Department of Electronic and Communication Engineering, Delhi Technological University, Delhi in partial fulfilment of the requirement for the award of the degree of Bachelor of Technology, is original and not copied from any source without proper citation. This work has not previously formed the basis for the award of any degree, Diploma Associateship, Fellowship or other similar title or recognition.

Place: Delhi

Date: 31 May, 2024

Piyush Kumar Singh(2K20/EC/144)

Rohit Singh (2K20/EC/171)

Rudra (2K20/EC/172)

DELHI TECHNOLOGICAL UNIVERSITY

(Formerly Delhi College of Engineering)

Bawana Road, Delhi-110042

CERTIFICATE

I hereby certify that the Project Dissertation titled "**UWB Share-Aperture Antenna for 5G Sub-6G Applications**" which is submitted by Piyush Kumar Singh (2K20/EC/144), Rohit Singh (2K20/EC/171) and Rudra (2K20/EC/172) students of B. Tech. Department of Electronic and Communication Engineering, Delhi Technological University, Delhi in partial fulfilment of the requirement for the award of the degree of Bachelor of Technology, is a record of the project work carried out by the students under my supervision. To the best of my knowledge this work has not been submitted in part or full for any Degree or Diploma to this University or elsewhere.

Place: Delhi

Date:22 May, 2024

Dr. PRIYANKA JAIN

SUPERVISOR

DELHI TECHNOLOGICAL UNIVERSITY

(Formerly Delhi College of Engineering)

Bawana Road, Delhi-11004

ACKNOWLEDGEMENT

We wish to express our gratitude to all individuals who have contributed to the advancement of this project and offered valuable suggestions for its enhancement. Our appreciation extends to Professor Priyanka Jain, Department of Electronics and Communication Engineering.

We consider ourselves privileged to have a supervisor who promptly addressed our inquiries and provided guidance throughout the project's progression. Particularly, our heartfelt thanks are extended to our parents, whose blessings and unwavering support have been pivotal in achieving our objectives. This collaborative support network has knowingly contributed to the successful completion of our goals.

Place: Delhi

Date: 22 May,

Piyush Kumar Singh(2K20/EC/109)

Rohit Singh (2K20/EC/171)

Rudra (2K20/EC/172)

ABSTRACT

This brief presents a compact shared-aperture antenna suitable for 5G Sub-6G applications. The antenna supports pattern and polarization diversity and uses coplanar waveguide (CPW) structures to activate monopole antennas through even modes and Vivaldi antennas through odd modes. A defected ground structure (DGS) is integrated to improve gain while minimizing back radiation and edge effects. By adjusting the excitation amplitude and phase at two ports, the antenna operates in four distinct modes: omnidirectional (mode 1), broadside (Mode-2), left tilted (mode 3), and right tilted (Mode-4). The antenna's dimensions are $0.667\lambda_0 \times 0.500\lambda_0 \times 0.007\lambda_0$, where λ_0 represents the free space wavelength at 2 GHz. These modes cover a 100 percent -10 dB impedance bandwidth (2-6 GHz). Within this common bandwidth (2-6 GHz, $|S11| < -10$ dB), the isolation between the two ports exceeds 25 dB. The design has been fabricated and tested, with measured results showing good agreement with the simulations.

TABLE OF CONTENTS

LIST OF TABLES

LIST OF FIGURES

CHAPTER 1

INTRODUCTION

1.1 GENERAL

The Sub-6 GHz spectrum is crucial in mobile communication for its wider coverage, lower propagation loss, reduced need for base stations, and extended transmission range. With the widespread adoption of 5G, beam-steering techniques in phased array antennas are advancing, enabling precise beam shaping and high-quality data transmission. However, phased arrays are expensive and complex, requiring numerous elements and phase shifters, along with challenging signal processing. As an alternative, pattern/polarization diversity is frequently employed for its simplicity and cost-effectiveness. Dipole, monopole, and patch antennas are commonly used for this purpose. Additionally, shared-aperture techniques in full-duplex systems enhance port isolation and pattern diversity performance, further optimizing communication.

1.2 COMPARISON WITH OTHER TECHNOLOGIES

Pattern reconfigurable antennas utilizing hybrid metamaterials are in [11] and [12]. These antennas offer versatility in adjusting their radiation patterns, enhancing communication performance. Additionally, multi-mode microstrip antennas are a viable option for achieving pattern diversity, as discussed in [13], [14], and [15]. These antennas can operate in different modes, providing flexibility in adapting to various communication scenarios and optimizing signal propagation. Researchers often manipulate PIN diodes to generate omnidirectional, broadside, or tilted antenna patterns in pattern diversity antenna designs, as noted in [16] and [17]. However, the limited operating range of PIN diodes poses constraints on these antennas. In [18], a compact monopole antenna is , leveraging defected ground structures (DGS), parasitic elements, and grounded branches to achieve compact size, high port isolation, and excellent diversity performance. Despite their potential in 5G mobile applications, these antennas face bandwidth limitations. In multiple-input multiple-output (MIMO) systems, wider bandwidth enhances channel capacity and information transmission in mobile communication. Therefore, there's a demand for compact broadband antennas with multiple patterns and polarizations to maximize diversity gain and transmission efficiency.

CHAPTER 2
LITERACY REVIEW

Research on monopole and Vivaldi antennas has a rich history, given their extensive use in various applications due to their distinct characteristics. Here is a detailed overview of the significant research and developments in both monopole and Vivaldi antennas:

2.1 MONOPOLE ANTENNA

2.1.2 Historical Development:

Monopole antennas, a type of radio antenna that consists of a single rod or conductor, have been widely studied since their inception. Initially, they were used in early radio communications and wireless telegraphy.

2.1.2 Design and Variations:

1. Basic Monopole Antennas: The classic quarter-wave monopole antenna is one of the simplest and most widely used forms. It typically consists of a single, vertical element mounted above a ground plane.

2. Folded Monopole Antennas: To improve bandwidth and impedance matching, folded monopole designs were developed. These include variants like the sleeve monopole, where additional conductive sleeves are used to enhance performance.

3. Planar Monopole Antennas: Advances in printed circuit technology led to the development of planar monopole antennas, which are used in compact and integrated systems, such as in mobile devices and WLAN applications.

2.1.3 Performance Enhancements:

1. Broadband Designs: Researchers have focused on broadening the bandwidth of monopole antennas. Techniques such as using tapered elements, adding parasitic elements, and employing different loading methods (e.g., inductive, capacitive) have been explored.

2. Miniaturization: For modern applications requiring compact designs, miniaturized monopole antennas have been studied extensively. Techniques include meandering the antenna element and using high-permittivity substrates.

2.1.4 Applications:

Monopole antennas are used in a wide range of applications, from simple radio receivers to complex systems in mobile communication, broadcasting, and radar.

2.2 VIVALDI ANTENNA

2.2.1 Historical Development:

Vivaldi antennas, a type of tapered slot antenna, were first introduced in the late 1970s. They are known for their wide bandwidth and high directivity.

2.2.2 Design and Variations:

1. Basic Vivaldi Antennas: The original Vivaldi antenna design consists of an exponentially tapered slot etched on a dielectric substrate. This design supports a wide range of frequencies and provides end-fire radiation.

2. Balanced Vivaldi Antennas: To improve the performance of Vivaldi antennas in certain applications, balanced designs were developed. These antennas have symmetric structures that help in reducing cross-polarization and improving pattern stability.

3. Planar and 3D Vivaldi Antennas: Modern fabrication techniques have allowed for both planar (2D) and three-dimensional (3D) implementations, expanding their use in various applications, including conformal and wearable systems.

2.2.3 Performance Enhancements:

1. Bandwidth and Gain Improvement: Researchers have explored various methods to enhance the bandwidth and gain of Vivaldi antennas. These include using different taper profiles, adding lens structures, and employing metamaterial substrates.

2. Array Configurations: Vivaldi antennas are often used in array configurations to achieve higher gain and more directional beams. Studies have focused on the design and optimization of Vivaldi antenna arrays for applications like radar, imaging, and phased array systems.

2.2.4 Applications:

Vivaldi antennas are used in applications requiring wide bandwidth and high directivity, such as in ultra-wideband (UWB) systems, ground-penetrating radar, microwave imaging, and communication systems.

2.3 COMPARATIVE RESEARCH AND COMBINED APPLICATIONS

2.3.1 Integration and Hybrid Designs:

In recent years, there has been interest in combining the characteristics of monopole and Vivaldi antennas to create hybrid designs that leverage the omnidirectional coverage of monopole antennas and the directional high-gain features of Vivaldi antennas. Research has focused on developing compact, versatile antennas capable of operating across multiple frequency bands, suitable for modern communication systems, including 5G and beyond.

2.3.2 Beam Steering and MIMO Systems:

Advancements in beam steering techniques and multiple-input multiple-output (MIMO) systems have also incorporated both monopole and Vivaldi antenna designs. Studies have explored the use of these antennas in smart antenna systems, where electronic steering of beams and adaptive radiation patterns are crucial for optimizing performance in dynamic environments.

2.3.3 Materials and Fabrication Techniques:

Ongoing research has also investigated new materials and fabrication techniques to enhance the performance of both monopole and Vivaldi antennas. This includes the use of advanced dielectric materials, metamaterials, and 3D printing technologies to create more efficient, compact, and robust antenna designs.

2.4 CURRENT RESEARCH

The current research focuses on the development and analysis of a Ultra-Wideband (UWB) Share-Aperture Antenna designed specifically for 5G Sub-6 GHz applications. Our work builds on the foundational principles of both monopole and Vivaldi antennas, integrating their distinct advantages into a single versatile antenna system capable of operating across multiple modes. Here's a detailed explanation of what has been accomplished in our research:

2.4.1 Design and Implementation

1. Hybrid Antenna Structure:

- Monopole Component: Incorporates vertical polarization and omnidirectional radiation characteristics. This component ensures broad and consistent coverage, essential for applications requiring uniform signal distribution.
- Vivaldi Component: Provides horizontal polarization with directional radiation. This component offers high directivity and efficiency for point-to-point communication links and focused beam applications.

2. Four Operational Modes:

- **Mode-1:** Utilizes the monopole antenna's omnidirectional pattern for extensive coverage. Ideal for base stations and broadcasting where uniform coverage is critical.
- **Mode-2:** Leverages the Vivaldi antenna's directional properties, achieving high gain and focused radiation suitable for targeted communication and radar applications.
- **Mode-3:** Introduces a 90° phase difference between ports, resulting in a left-tilted radiation pattern. This mode utilizes constructive and destructive interference to enhance radiation in specific directions, optimizing for scenarios requiring directional control.
- **Mode-4:** Implements a -90° phase difference, producing a right-tilted radiation pattern. This mode, similar to Mode 3, allows for beam steering capabilities through phase control, crucial for dynamic communication environments.

2.4.2 Analysis and Performance Evaluation

1. Current Distribution:

- **Mode-1:** Concentrated at the lower part, indicating strong resonance and efficient radiation at lower frequencies.
- **Mode-2:** Uniform distribution across the antenna surface, suggesting efficient radiation at a different frequency band, enhancing overall antenna efficiency.
- **Mode-3:** Concentrated towards the edges, indicating distinct radiation patterns and another resonance frequency, beneficial for directional applications.
- **Mode-4:** Balanced distribution, optimizing performance for various frequency bands, demonstrating the antenna's adaptability.

2. Radiation Patterns:

- **Mode-1:** Exhibits an omnidirectional pattern with vertical polarization, suitable for broad coverage.
- **Mode-2:** Shows a broadside radiation pattern with horizontal polarization, ideal for point-to-point communication.
- **Mode-3 and Mode-4:** Demonstrate tilted radiation patterns (left and right, respectively), achieved through phase differences. These patterns underscore the antenna's capability for beam steering, enhancing its utility in advanced communication systems.

3. Far-Field Gain Analysis:

- **Mode-1:** Gain of 2.95 dBi, providing moderate side lobe suppression and suitable for uniform coverage applications.
- **Mode-2:** Gain of 8.11 dBi, with significant side lobe suppression, ideal for focused, high-gain applications.
- **Mode-3:** Balanced gain and broader beam, offering a compromise between directivity and coverage area.
- **Mode-4:** Similar gain with the broadest beam, suitable for extensive coverage areas and environments requiring minimal interference.

2.5 CONTRIBUTIONS AND INNOVATIONS

Material Selection: In contrast to the prevalent use of aluminium in antenna design, copper was chosen for its distinct properties and potential performance benefits. The decision to utilize copper stemmed from its superior electrical conductivity, which theoretically promises enhanced antenna efficiency. However, the transition from aluminium to copper presented formidable obstacles, primarily stemming from the intrinsic properties of copper.

This thesis explores the utilization of copper, a less conventional material in antenna design, over the commonly used aluminium, to achieve superior performance. While aluminium has been traditionally favoured for its availability and conductivity, the adoption of copper poses challenges that demand innovative solutions for optimal results.

Substrate Optimization: Copper was selected for its distinct properties and potential performance benefits. The decision to employ copper stemmed from its superior electrical conductivity, promising enhanced antenna efficiency. However, the transition from aluminium to copper necessitated innovative solutions to overcome fabrication and tuning challenges.

Simultaneously, the substrate material played a critical role in antenna performance. Departing from the common choice of FR4, which is known for its inherent losses, a shift was made towards a less conventional, less lossy substrate material. This strategic decision aimed to minimize losses and maximize antenna efficiency, albeit with additional complexities in fabrication and tuning.

Innovative DGS Implementation: In addition to material considerations. This thesis delves into a multi-faceted approach to antenna enhancement, combining the utilization of copper, optimization of substrate material, and the innovative integration of slot cutting along with circular cutting for Defected Ground Structure (DGS). Departing from conventional practices, this research embodies a spirit of innovation and exploration, aiming to push the boundaries of antenna engineering to achieve unprecedented performance levels this thesis introduces a novel approach to antenna design through the integration of slot cutting along with circular cutting for Defected Ground Structure (DGS). This innovative technique aims to mitigate surface wave propagation and enhance antenna performance by introducing localized perturbations in the ground plane. The synergistic combination of slot cutting and circular cutting offers a unique avenue for achieving superior antenna characteristics, demanding meticulous design and optimization efforts.

Challenges and Solutions: Designing an antenna with copper and optimizing the substrate material posed formidable challenges. The higher conductivity of copper and the complexities associated with the new substrate demanded meticulous attention to detail and precision in design. Imperfections in fabrication or substrate selection could significantly impact antenna performance, necessitating innovative approaches to mitigate these challenges The introduction of slot cutting and circular cutting for DGS presents a new set of challenges in antenna design. Precise control over the dimensions and placement of slots and circular cuts is paramount to achieving the desired performance improvements. Moreover, the interaction between these features and other antenna elements necessitates thorough analysis and iterative refinement to optimize performance while minimizing undesired effects.

CHAPTER 3
ANTENNA AND FEEDER DESIGN

3.1 CONFIGURATION OF ANTENNA

The suggested antenna's concrete construction is illustrated in Fig. 3, comprising two metal layers: a yellow top layer and a blue bottom layer, both printed on an F4R substrate ($\varepsilon_r = 4.3$, $\tan\delta = 0.0025$) with a thickness of 1 mm. The CPW structure's even and odd modes are activated by two ports. In Fig. 3, port 1 excites the even mode, generating a vertical polarization due to in-phase excitation of the E-field distribution. Conversely, port 2 excites the odd mode, producing a horizontal polarization through out-of-phase excitation of the E-field distribution. The establishment of orthogonal polarizations naturally yields excellent port isolation.

Table 1 Dimensions of the Antenna

Parameter	(mm)	Parameter	(mm)
A	75	B	100
C	40.13	D	1
R1	42.8	R2	15.86

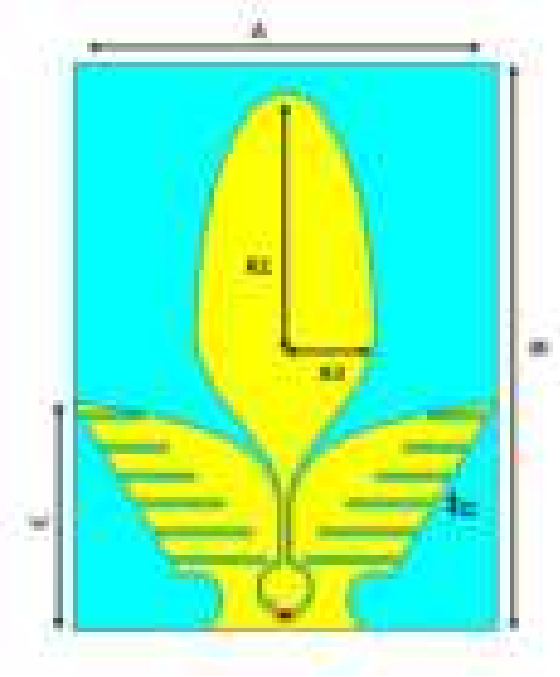

Fig.3 Geometry of the Antenna

3.2 ANTENNA DESIGN GUIDELINE

The antenna design procedure, as illustrated in Fig. 1, begins with the creation of two distinct antennas: a monopole and a Vivaldi antenna. The monopole is specifically designed to enable vertical polarization and omnidirectional radiation patterns, making it ideal for applications where signal coverage in all directions is essential. Conversely, the Vivaldi antenna is crafted for horizontal polarization and broadside radiation patterns, which are crucial for focused signal transmission and reception. Both antennas are designed to exhibit ultra-wideband (UWB) properties, ensuring they can operate efficiently over a wide frequency range.

Following the individual development of these antennas, they are integrated to form Antenna 1. This integration leverages the complementary features of the monopole and Vivaldi antennas, resulting in a versatile antenna system. To further enhance the performance of Antenna 1, a defected ground structure (DGS) is incorporated into the design. The DGS serves to increase the antenna's gain and reduce unwanted back radiation and edge effects, which can degrade performance. This structural modification not only improves the antenna's efficiency but also enhances its overall radiation characteristics, making it suitable for advanced communication systems requiring high gain and minimal interference. The resulting antenna system, with its combined UWB capabilities and optimized design, is poised to deliver superior performance in a variety of applications.

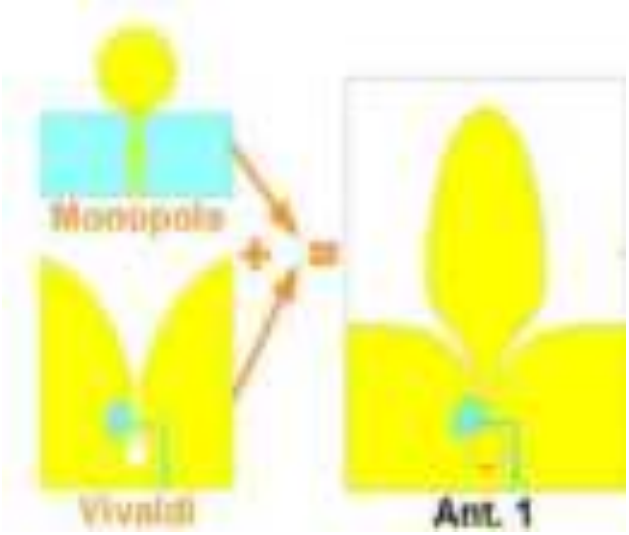

Fig 4. Combination of Monopole and Vivaldi Antenna

3.3 OPERATING MODES OF THE ANTENNA

Table 2 Four modes of the antenna.

Modes	Port 1	Port 2	BW (GHz)
Mode-1	1	0	1.17–7
Mode-2	0	1	1.9–5.9
Mode-3	1 (0)	1 (90)	1.16–7.06
Mode-4	1 (0)	1 (-90)	1.14–7.13

The antenna design involves multiple operating modes, each defined by different configurations of inputs at Port 1 and Port 2, which subsequently affect the bandwidth (BW) over which the antenna operates efficiently. These modes are tailored to enhance the versatility and functionality of the antenna system across a range of frequencies.

Mode-1 is characterized by an active signal at Port 1 while Port 2 is inactive (Port 1 = 1, Port 2 = 0). In this configuration, the antenna operates over a wide bandwidth ranging from 1.17 GHz to 7 GHz. This mode is likely leveraged for applications requiring extensive frequency coverage and robust performance across this broad spectrum.

Mode-2 switches the active port to Port 2 while Port 1 remains inactive (Port 1 = 0, Port 2 = 1). The operational bandwidth in this mode is slightly narrower, spanning from 1.9 GHz to 5.9 GHz. This configuration could be optimized for scenarios where specific frequency bands within this range are of particular interest, providing flexibility depending on the application requirements.

Mode-3 introduces a different operational dynamic, where both ports are active with Port 1 and Port 2 receiving signals at the same phase (Port 1 = 1, Port 2 = 1) but with Port 2 phase-shifted by 90 deg. relative to Port 1 (denoted as 1 (0) and 1 (90)). This mode supports a bandwidth from 1.16.00 GHz to 7.06.00 GHz. The phase difference between the ports suggests this mode is designed to exploit polarization diversity or other advanced antenna techniques, enhancing performance in environments where multipath interference is a concern.

Mode-4 is similar to Mode-3 in that both ports are active, but with Port 2 phase-shifted by -90 deg. relative to Port 1 (denoted as 1 (0) and 1 (-90)). This also results in an operational bandwidth from 1.14 GHz to 7.13 GHz. The phase shift in the opposite direction compared to Mode-3 likely provides additional capabilities for managing polarization states or beamforming, optimizing the antenna for specific communication scenarios.

.

3.4 OPERATING MECHANISM OF THE ANTENNA

The antenna features a symmetrical design, ensuring balanced current distribution when one port is active and the other is matched. This balance is crucial as it prevents the radiation patterns from tilting, maintaining stable and predictable performance. Figure 5 illustrates the simulated surface current distributions for the different modes of operation, showcasing the antenna's versatility in handling various polarization and radiation pattern requirements.

In Mode-1, where Port 1 is active and Port 2 is matched (Port 1 = 1, Port 2 = 0), the antenna exhibits vertical polarization. This mode leverages the monopole component of the antenna, resulting in omnidirectional radiation patterns. This means the antenna radiates equally in all directions along the horizontal plane, making it ideal for applications requiring uniform coverage, such as broadcasting or general communication networks where signal reception is needed from multiple directions.

Mode-2 involves activating Port 2 while Port 1 is matched (Port 1 = 0, Port 2 = 1). In this configuration, the antenna demonstrates horizontal polarization, with broadside radiation patterns. This behavior is predominantly due to the Vivaldi component of the antenna, which focuses the radiation in a broadside direction (perpendicular to the axis of the antenna). This mode is particularly useful for applications requiring directed signals, such as point-to-point communication links, where a focused beam can improve signal strength and reduce interference.

Modes 3 and 4 are more complex, involving simultaneous activation of both ports but with phase differences between them. These modes essentially combine the behaviors of two symmetrical Vivaldi antennas. In Mode-3, a 90° phase difference is introduced between Port 2 and Port 1 (Port 1 = 1 (0), Port 2 = 1 (90)). This phase difference creates an imbalance in the current distribution. The resulting current and electric field (E-field) in the left Vivaldi antenna aperture superimpose constructively, while they cancel out in the right aperture. This superposition causes the radiation pattern to tilt to the left. Such tilted patterns are advantageous for applications like direction finding or beam steering, where controlling the direction of the main lobe is critical.

Conversely, Mode-4 introduces a -90° phase difference between Port 2 and Port 1 (Port 1 = 1 (0), Port 2 = 1 (-90)). This phase configuration leads to the opposite effect: the currents and E-field in the right Vivaldi antenna aperture superimpose, while they cancel out on the left, producing a right-tilted radiation pattern. This mode can be used similarly to Mode-3 but for targeting directions on the opposite side, offering further flexibility in controlling the radiation direction.

The symmetrical design of the antenna and its ability to switch between these modes without causing unwanted pattern tilting is a significant advantage. By maintaining balanced current distributions when either port is active alone, the antenna ensures stable radiation characteristics. The introduction of phase differences in Modes 3 and 4 allows for precise control over the directionality of the radiation pattern, making the antenna highly adaptable for various advanced communication scenarios. This ability to dynamically adjust the radiation pattern and polarization based on the operational mode makes the antenna an excellent choice for modern communication systems that demand high performance and versatility.

3.5 DESIGN FOR FEEDER

3.5.1 Wilkinson Power Divider Basics:

The Wilkinson power divider, also known as the Wilkinson power divider, is a commonly used passive component in RF and microwave systems, including in the design of antenna feed systems. It's often employed as part of the stage 1 antenna feeder to split an incoming RF signal into two or more equal or unequal parts with minimal loss and impedance mismatch.

Table 3 Dimension of the Feeder

Parameter	(mm)
P	50
Q	40

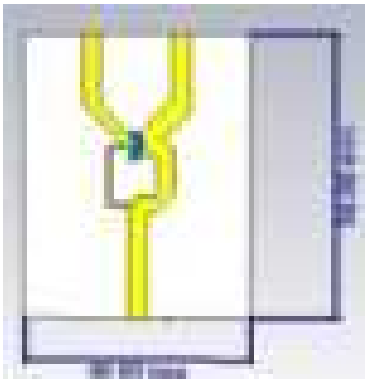

Fig. 5 Feeder for operating Mode 3 & 4 of antenna

- **Functionality**: The Wilkinson power divider is a type of resistive power divider that uses quarter-wavelength transmission line sections and resistors to divide the input power into multiple output ports. It provides isolation between the output ports and typically exhibits excellent impedance matching properties.
- **Operation**: At its core, the Wilkinson power divider consists of a hybrid junction formed by a quarter-wavelength transmission line connected to two resistors. When an RF signal is applied to the input port, it divides equally between the two output ports while maintaining a matched impedance at all ports. The resistors terminate the unused port, ensuring impedance matching and minimizing reflections.

- **Design Considerations**:
    - Design parameters such as the characteristic impedance of the transmission lines and the values of the resistors determine the performance of the Wilkinson power divider.

- Proper impedance matching and isolation between the output ports are critical design considerations.

3.4.2 Application in Stage 1 Antenna Feeder:

- **Signal Distribution**:
  - In the context of the stage 1 antenna feeder, the Wilkinson power divider can be used to split the RF signal from the transmitter into multiple branches, each feeding a separate antenna element or array.
  - This allows for the implementation of antenna systems with multiple elements or beams, such as phased array antennas or antenna diversity systems.
- **Balancing Network**:
  - The Wilkinson power divider serves as a balancing network, ensuring that each antenna element receives the appropriate level of RF power while maintaining impedance matching.
  - This is particularly important in phased array systems where precise control of the relative phase and amplitude of the signals feeding each element is necessary to steer the antenna beam.
- **Loss and Efficiency**:
  - The Wilkinson power divider introduces some loss due to the resistive terminations, but it is typically low compared to other power dividing techniques.
  - By minimizing losses and maintaining impedance matching, the Wilkinson power divider contributes to the overall efficiency of the stage 1 antenna feeder and the antenna system as a whole.

3.4.3 Advantages:

- **Broadband Operation**:
  - The Wilkinson power divider can operate over a wide frequency range, making it suitable for broadband antenna systems and multi-band applications.
  - Its performance is relatively insensitive to frequency variations within its operational bandwidth.
- **Simple Construction**: The Wilkinson power divider can be implemented using standard transmission line and resistor components, making it relatively simple and cost-effective to manufacture.
- **Robustness**: Due to its passive nature and simple construction, the Wilkinson power divider is inherently robust and reliable, with no active components to fail or require maintenance.

CHAPTER 4
FABRICATION

Before going to fabricate antenna, we need to follow some proper steps which we had performed in our antenna fabrication.

4.1 DESIGN PHASE:

Determine the desired operating frequency, gain, bandwidth, polarization, and other performance parameters. Select the appropriate antenna type based on the application and requirements (e.g., Monopole, Vivaldi). Use the simulation software CST Because I had also used CST.

One of the most precious steps here is that we need to be careful while doing this because it will help us to achieve the desired results.

4.1.1 Material Selection:

Choose substrate material: Select a substrate material with suitable dielectric properties, and also after confirming the availability of it in our lab such as FR4. Select conductive material: Choose a conductive material for the antenna elements, typically copper or aluminium.

4.1.2 Gerber File Preparation:

- Once we complete the software part after that we need to create Gerber files of that design for the next process.
- Ensure that your Gerber files are correctly generated and the axis alignment should like that:-

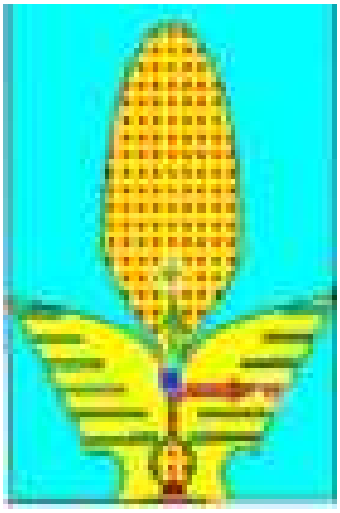

Fig.6 Axis Alignment

- Verify that the Gerber files are free from errors or anomalies that could affect the PCB fabrication process.

4.2 MANUAL PHOTOLITHOGRAPHY

Photolithography is commonly used for fabricating printed circuit board (PCB) antennas, such as microstrip antennas.

4.2.1 Film Printing:

Print each positive film layer onto transparent film sheets using a high-resolution film printer or a laser photoplotter. Ensure that the films are printed with high precision and accuracy to accurately represent the PCB design features.

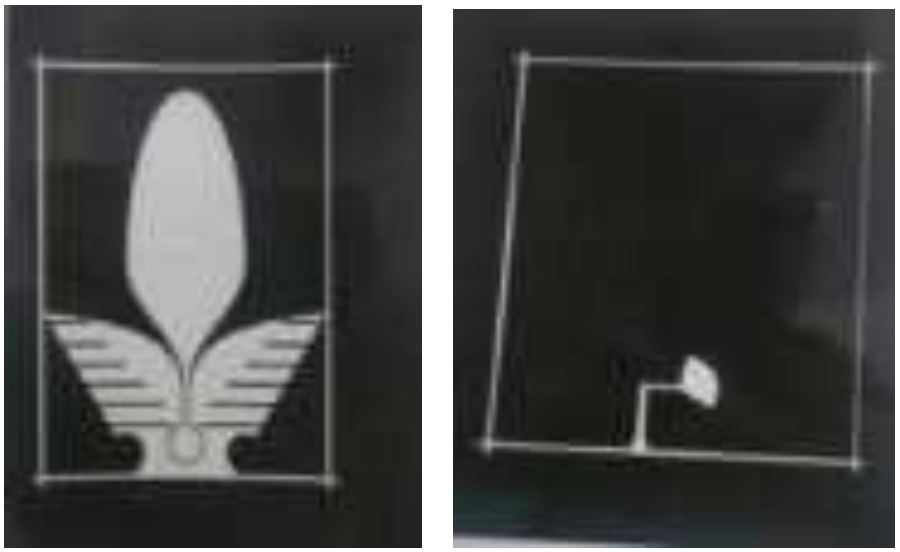

(a) (b)

Fig. 7. Film Mask (a) Top Layer (b) Bottom Layer

4.2.2 Exposure Process:

i. **Negative Film Preparation:** Obtain clear acetate sheets or transparent film sheets to serve as the base for negative films.

ii. **Coating Application**: Apply a thin, even layer of photosensitive emulsion or film onto one side of the acetate sheet using a coating machine or manual spreading technique. Ensure that the emulsion layer is uniform and free from bubble that could degrade the quality of the negative films.

iii. **Film Exposure**: Place the positive film layers onto the coated side of the acetate sheets, ensuring proper alignment and registration with the emulsion-coated surface. Expose the film assembly to UV lightbox for a specified duration, typically determined by the sensitivity of the emulsion and the desired level of image resolution.

iv. **Development**: Remove the positive films from the acetate sheets after exposure, leaving behind latent images of the PCB design features on the emulsion-coated surface. Develop the exposed acetate sheets in an alkaline developer solution to reveal the latent images and convert them into opaque negative images.

v. **Fixing and Drying**: Fix the developed acetate sheets in a fixing solution to remove any unexposed emulsion and stabilize the negative images. Rinse the fixed acetate sheets with water to remove residual chemicals and then allow them to air-dry thoroughly before further handling.

vi. **Overlay Alignment**: Align and register the negative films with each other and with the corresponding layers of the PCB substrate to ensure accurate layer-to-layer alignment during PCB fabrication.

vii. **PCB Fabrication:** Use the negative films to create photoresist masks or stencils for various PCB fabrication processes, etching, solder mask application.

4.2.3 Quality Control:

Perform quality control checks on the fabricated PCBs to verify that they meet the design specifications and performance requirements.

Fig. 8 Used ink to protect required copper from etching.

Results during Etching

- In our first go we didn't get the perfect etching but we tried one more time the same process we got perfect etching.

Fig. 9(a). Rough etched design

Fig. 9(b). Left is manually etched design and Right is CNC etched design

Finally, we had fabricated the desired design for future implementation and for application. And also compared the CNC and manual Etched design both are perfect but the manual took a lot of effort and CNC did within the hour.

4.3 FABRICATION USING CNC MACHINE

4.3.1 CNC Machine Setup

- **Load Material:**Secure the material onto the CNC machine's worktable using clamps or a vacuum table.
- **Install Tools:** Install the necessary cutting tools, such as end mills, drills, and engraving bits, into the CNC machine.
- **Calibrate Machine:** Calibrate the machine by setting the zero points for the X, Y, and Z axes.

4.3.2 Cutting and Shaping

- **Start Machining:** Execute the CNC program generated from the CAM software. The machine will follow the programmed toolpaths to cut, mill, drill, and shape the material into the desired antenna structure.
- **Monitor Process:** Continuously monitor the machining process to ensure precision and make adjustments if necessary.

4.3.3 Assembly (if required)

If the antenna design includes multiple parts, assemble them using appropriate methods such as soldering, welding, or using mechanical fasteners to ensure proper alignment and secure connections.

4.3.4 Finishing

Perform surface finishing processes by putting it into FeCl3 solution for etching so all the unwanted copper will get removed

4.3.5 Quality Assurance

Conduct a thorough inspection to ensure the antenna meets all design specifications and quality standards. Document the design, fabrication process, and test results for future reference and certification purposes.

(a) (b)

Fig. 10 Final Design of Antenna using CNC Machine (a) Top Layer (b) Bottom Layer

CHAPTER 5

RESULTS

5.1 SIMULATED RESULT

5.1.1 S Parameter

The S-parameter, or scattering parameter, is essential in antenna design and analysis, particularly S_{11} which measures the return loss or reflection coefficient. It indicates how much input power is reflected back to the source, with lower values signifying better impedance matching and more efficient performance. Engineers aim for an S_{11} value below -10 dB to ensure minimal signal reflection and maximal power transmission. These parameters are crucial for optimizing antenna performance, ensuring proper impedance matching, and are typically measured using network analyzers and visualized on Smith Charts.

Mode-1

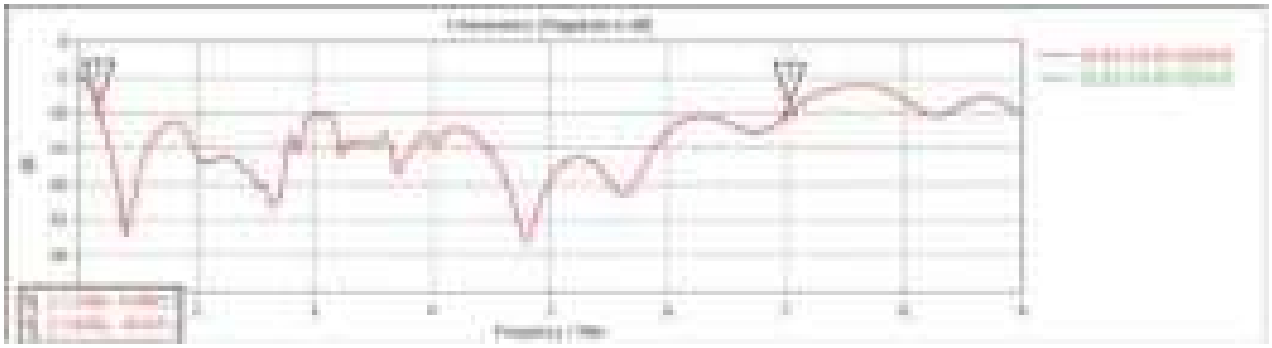

Fig. 11 (a) Simulated Results - S parameter - Mode-1

The provided graph displays the S-parameters (magnitude in dB) for Mode-1 of the antenna, covering a frequency range from 1 GHz to 9 GHz. This mode is characterized by Port 1 being active with a configuration of [1.0, 0.0, 0.0] and Port 2 being matched with [0.0, 0.0]. The graph shows two parameters: S_{11} (in red) and S_{21} (in green), but in this particular screenshot, the focus is on S_{11}.

Analysis of the S-Parameter Graph Fig. 11 (a) i.e Mode-1

Low-Frequency Range (1-2 GHz):

- At around 1.1764 GHz, S_{11} dips to approximately -9.9997 dB. This indicates that at this frequency, the antenna exhibits reasonable impedance matching with a return loss close to -10 dB, which is a common benchmark for acceptable performance. The highlighted point (Q1) on the graph confirms this measurement.
- The graph shows significant variation in the S-parameter within this low-frequency range, suggesting multiple resonances and transitions where the antenna's impedance matching fluctuates.

Mid-Frequency Range (2-5 GHz):

- The S_{11} parameter exhibits several peaks and troughs, indicating varying deg. of impedance matching and reflection. The antenna demonstrates several resonant frequencies within this range where the return loss improves (dips in the graph).
- Around the mid-range frequencies, the dips are not as pronounced as in the lower range, but multiple frequencies show values below -10 dB, suggesting good performance at these points.

High-Frequency Range (5-9 GHz):

- Notable dips in the S_{11} parameter occur again around 7.0256 GHz, where the return loss reaches -10.025 dB (highlighted point Q2). This indicates another point of good impedance matching, essential for efficient operation at higher frequencies.
- The overall trend in this high-frequency range shows less fluctuation compared to the lower ranges, indicating more stable impedance matching performance.

Specific Points of Interest:

1. Highlighted Points (Q1 and Q2):

- Q1 (1.1764 GHz, -9.9997 dB): This point shows where the antenna achieves close to -10 dB return loss in the low-frequency range, indicating relatively good performance.
- Q2 (7.0256 GHz, -10.025 dB): In the higher frequency range, this point also shows a return loss around -10 dB, indicating efficient performance.

2. General Performance:

- Across the entire frequency range, the antenna shows multiple frequencies where S_{11} dips below -10 dB, indicating good impedance matching and low reflection at these points.
- The peaks where S_{11} values are higher (less negative) indicate frequencies where the antenna is not as well matched, resulting in higher reflection and less efficient performance.

Implications for Antenna Performance:

- **Wideband Operation:** The multiple dips below -10 dB across the frequency spectrum confirm the antenna's wideband capabilities, making it suitable for applications requiring broad frequency coverage.
- **Efficiency:** Points where S_{11} reaches values around -10 dB or lower indicate frequencies where the antenna performs efficiently, with minimal power loss due to reflection.
- **Design Optimization:** The data from the S-parameter graph can be used to further optimize the antenna design, focusing on minimizing peaks where the return loss is higher to achieve better overall performance across the desired frequency range.

Mode-2

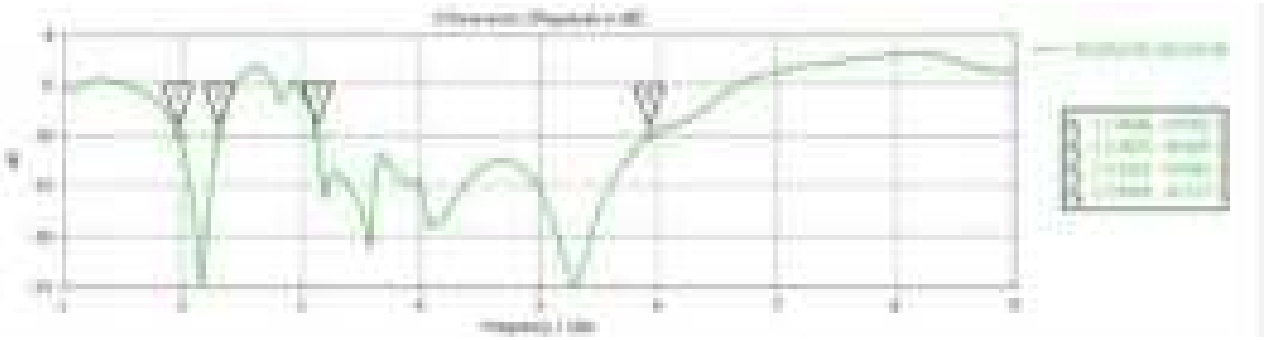

Fig. 11 (b) Simulated Results - S parameter - Mode-2

The provided graph displays the S-parameters (magnitude in dB) for Mode-2 of the antenna, covering a frequency range from 1 GHz to 9 GHz. In this mode, Port 2 is active with a configuration of [1.0, 0.0, 0.0] while Port 1 is matched with [0.0, 0.0]. The graph shows the S_{21} parameter, indicating how power is transmitted from Port 1 to Port 2.

Analysis of the S-Parameter Graph Fig. 11 (b) i.e Mode-2

Low-Frequency Range (1-2 GHz):

- At around 1.9628 GHz, S_{21} dips to approximately -9.9762 dB. This indicates that at this frequency, the antenna exhibits reasonable impedance matching with a return loss close to -10 dB, which is a common benchmark for acceptable performance. The highlighted point (Q1) on the graph confirms this measurement.
- The graph shows significant variation in the S-parameter within this low-frequency range, suggesting multiple resonances and transitions where the antenna's impedance matching fluctuates.

Mid-Frequency Range (2-5 GHz):

- The S_{21} parameter exhibits several peaks and troughs, indicating varying deg. of impedance matching and reflection. The antenna demonstrates several resonant frequencies within this range where the return loss improves (dips in the graph).
- Notable dips occur at:
  - - 2.3077 GHz, where S_{21} reaches -10.035 dB (Q2)
  - - 3.1317 GHz, with a value of -9.9381 dB (Q3)
- These points indicate frequencies where the antenna performs well, with good impedance matching and low reflection.

High-Frequency Range (5-9 GHz):

- In the higher frequency range, a notable dip in the S_{21} parameter occurs around 5.9209 GHz, where the return loss reaches -10.117 dB (highlighted point Q4). This indicates another point of good impedance matching, essential for efficient operation at higher frequencies.
- The overall trend in this high-frequency range shows less fluctuation compared to the lower ranges, indicating more stable impedance matching performance.

Specific Points of Interest:

1. Highlighted Points (Q1 to Q4):

- Q1 (1.9628 GHz, -9.9762 dB): This point shows where the antenna achieves close to -10 dB return loss in the low-frequency range, indicating relatively good performance.
- Q2 (2.3077 GHz, -10.035 dB): Shows good performance in the lower mid-frequency range.
- Q3 (3.1317 GHz, -9.9381 dB): Indicates a point of good impedance matching in the mid-frequency range.
- Q4 (5.9209 GHz, -10.117 dB): Demonstrates efficient performance at a higher frequency.

2. General Performance:

- Across the entire frequency range, the antenna shows multiple frequencies where S_{21} dips below -10 dB, indicating good impedance matching and low reflection at these points.
- The peaks where S_{21} values are higher (less negative) indicate frequencies where the antenna is not as well matched, resulting in higher reflection and less efficient performance.

Implications for Antenna Performance:

- **Wideband Operation:** The multiple dips below -10 dB across the frequency spectrum confirm the antenna's wideband capabilities, making it suitable for applications requiring broad frequency coverage.
- **Efficiency:** Points where S_{21} reaches values around -10 dB or lower indicate frequencies where the antenna performs efficiently, with minimal power loss due to reflection.
- **Design Optimization:** The data from the S-parameter graph can be used to further optimize the antenna design, focusing on minimizing peaks where the return loss is higher to achieve better overall performance across the desired frequency range.

Mode-3

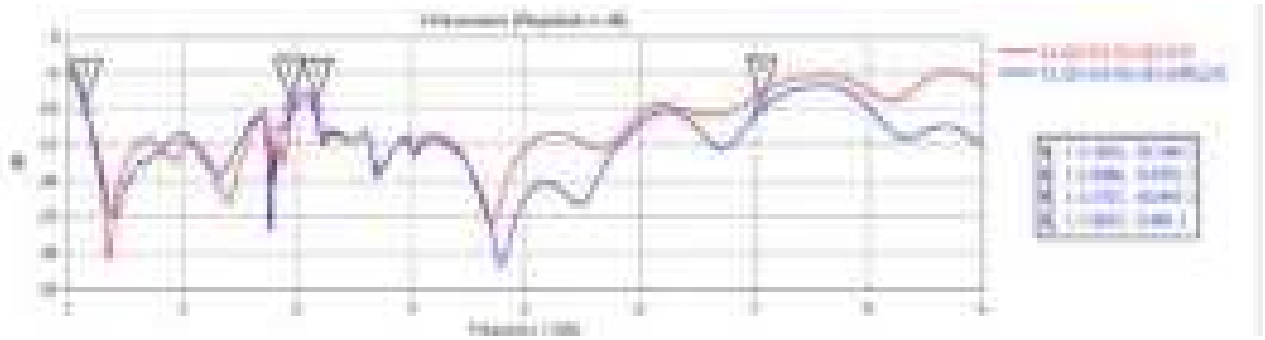

Fig. 11 (c) Simulated Results - S parameter - Mode-3

Analysis of the S-Parameter Graph for Fig. 11 (c) i.e Mode-3

Low-Frequency Range (1-2 GHz):

- At around 1.1601 GHz, S_{11} dips to approximately -10.206 dB (highlighted point 1). This indicates that at this frequency, the antenna exhibits reasonable impedance matching with a return loss close to -10 dB, which is a common benchmark for acceptable performance.
- The graph shows significant variation in the S-parameter within this low-frequency range, suggesting multiple resonances and transitions where the antenna's impedance matching fluctuates.

Mid-Frequency Range (2-5 GHz):

- At 2.9386 GHz, S_{11} dips to approximately -9.9791 dB (highlighted point 2), indicating a point of good impedance matching. Similarly, at 3.1717 GHz, the return loss reaches -10.042 dB (highlighted point 3). These points demonstrate that the antenna achieves good performance at multiple mid-range frequencies.
- The S-parameter exhibits several peaks and troughs, indicating varying deg. of impedance matching and reflection within this range. Despite the fluctuations, the antenna shows good performance at specific frequencies where the return loss dips below -10 dB.

High-Frequency Range (5-9 GHz):

- At 7.0697 GHz, S_{11} dips to approximately -9.901 dB (highlighted point 4). This indicates another point of good impedance matching in the high-frequency range.
- The overall trend in this high-frequency range shows less fluctuation compared to the lower ranges, indicating more stable impedance matching performance.

Specific Points of Interest:

1. **Highlighted Points:**
   - Point 1 (1.1601 GHz, -10.206 dB): This point shows where the antenna achieves good return loss in the low-frequency range, indicating relatively good performance.
   - Point 2 (2.9386 GHz, -9.9791 dB): In the mid-frequency range, this point indicates good impedance matching.
   - Point 3 (3.1717 GHz, -10.042 dB): Another mid-frequency point of good performance.
   - Point 4 (7.0697 GHz, -9.901 dB): In the higher frequency range, this point also shows a return loss around -10 dB, indicating efficient performance.

2. **General Performance:**
   - Across the entire frequency range, the antenna shows multiple frequencies where S_{11} dips below -10 dB, indicating good impedance matching and low reflection at these points.
   - The peaks where S_{11} values are higher (less negative) indicate frequencies where the antenna is not as well matched, resulting in higher reflection and less efficient performance.

Implications for Antenna Performance:

- **Wideband Operation:** The multiple dips below -10 dB across the frequency spectrum confirm the antenna's wideband capabilities, making it suitable for applications requiring broad frequency coverage.
- **Efficiency:** Points where S_{11} reaches values around -10 dB or lower indicate frequencies where the antenna performs efficiently, with minimal power loss due to reflection.
- **Design Optimization:** The data from the S-parameter graph can be used to further optimize the antenna design, focusing on minimizing peaks where the return loss is higher to achieve better overall performance across the desired frequency range.

Mode-4

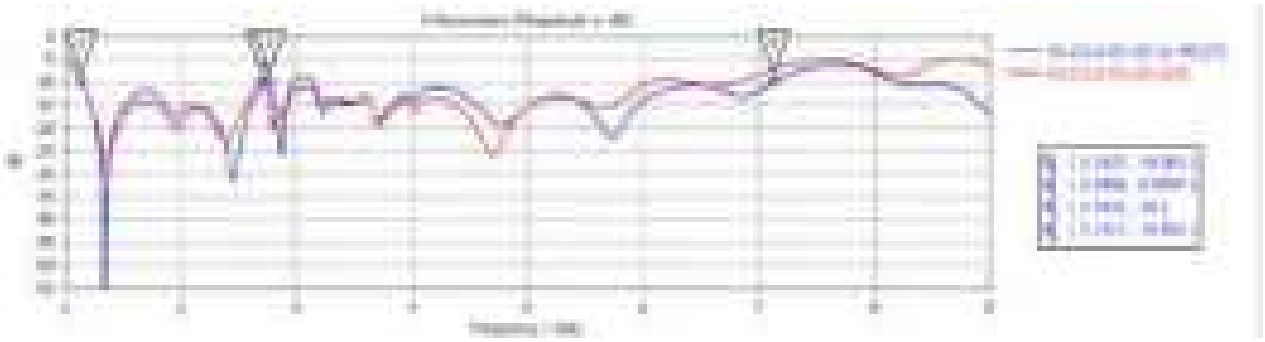

Fig 11 (d) Simulated Results - S parameter - Mode-4

Analysis of the S-Parameter Graph for Fig. 11 (d) i.e Mode 4

Low-Frequency Range (1-2 GHz):

- At around 1.1427 GHz, S_{11} dips to approximately -10.001 dB (highlighted point 1). This indicates that at this frequency, the antenna exhibits good impedance matching with a return loss close to -10 dB, which is a common benchmark for acceptable performance.

- The graph shows significant variation in the S-parameter within this low-frequency range, suggesting multiple resonances and transitions where the antenna's impedance matching fluctuates.

Mid-Frequency Range (2-5 GHz):

- At 2.6996 GHz, S_{11} dips to approximately -9.9994 dB (highlighted point 2), indicating a point of good impedance matching. Similarly, at 2.7631 GHz, the return loss reaches -10 dB (highlighted point 3). These points demonstrate that the antenna achieves good performance at multiple mid-range frequencies.

- The S-parameter exhibits several peaks and troughs, indicating varying deg. of impedance matching and reflection within this range. Despite the fluctuations, the antenna shows good performance at specific frequencies where the return loss dips below -10 dB.

High-Frequency Range (5-9 GHz):

- At 7.1317 GHz, S_{11} dips to approximately -10.001 dB (highlighted point 4). This indicates another point of good impedance matching in the high-frequency range.The overall trend in this high-frequency range shows less fluctuation compared to the lower ranges, indicating more stable impedance matching performance.

Specific Points of Interest:

1. **Highlighted Points:**
   - Point 1 (1.1427 GHz, -10.001 dB): This point shows where the antenna achieves good return loss in the low-frequency range, indicating relatively good performance.
   - Point 2 (2.6996 GHz, -9.9994 dB): In the mid-frequency range, this point indicates good impedance matching.
   - Point 3 (2.7631 GHz, -10 dB): Another mid-frequency point of good performance.
   - Point 4 (7.1317 GHz, -10.001 dB): In the higher frequency range, this point also shows a return loss around -10 dB, indicating efficient performance.
2. **General Performance:**

   Across the entire frequency range, the antenna shows multiple frequencies where S_{11} dips below -10 dB, indicating good impedance matching and low reflection at these points.

   The peaks where S_{11} values are higher (less negative) indicate frequencies where the antenna is not as well matched, resulting in higher reflection and less efficient performance.

Implications for Antenna Performance:

- **Wideband Operation:** The multiple dips below -10 dB across the frequency spectrum confirm the antenna's wideband capabilities, making it suitable for applications requiring broad frequency coverage.
- **Efficiency:** Points where S_{11} reaches values around -10 dB or lower indicate frequencies where the antenna performs efficiently, with minimal power loss due to reflection.
- **Design Optimization:** The data from the S-parameter graph can be used to further optimize the antenna design, focusing on minimizing peaks where the return loss is higher to achieve better overall performance across the desired frequency range.

5.1.2 Polar Representation

The polar representation of an antenna's radiation pattern provides a detailed view of how electromagnetic energy is radiated or received by the antenna in various directions. This visualization is typically plotted in a polar coordinate system, where the azimuthal angle (horizontal angle) is represented along the circumference, ranging from 0 to 360 deg., and the elevation angle (vertical angle) is represented radially from the center.

The Fig. 12 (a), (b), (c), and (d) illustrate the polar radiation patterns of the Ultra-Wideband (UWB) Share-Aperture Antenna in four different modes, highlighting its ability to support diverse radiation characteristics essential for 5G Sub-6 GHz applications.

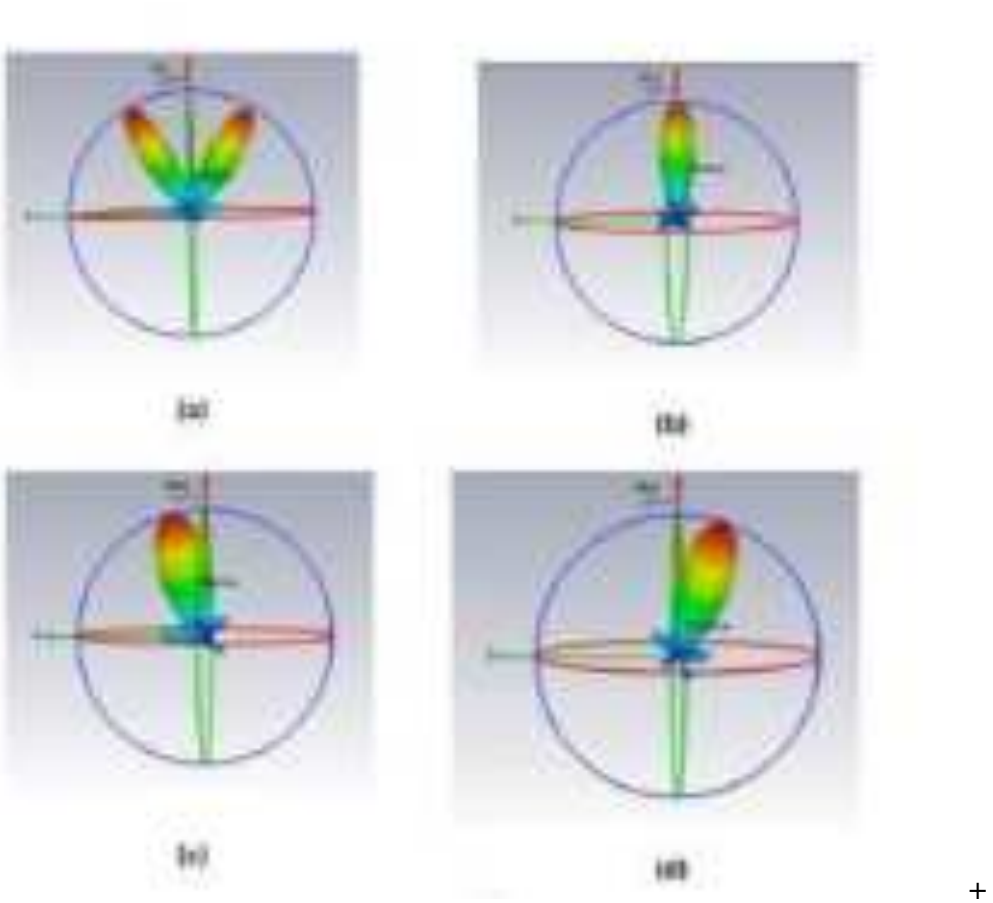

Fig. 12. Simulated Result - 3-D Radiation Pattern (a) Mode-1 (b) Mode-2 (c) Mode-3 (d) Mode-4

Mode-1 - Vertical Polarization with Omnidirectional Radiation

In Mode-1, as depicted in Figure 12 (a), the antenna exhibits vertical polarization and an omnidirectional radiation pattern. This pattern is characteristic of a monopole antenna, which provides consistent coverage across the entire azimuth plane. The radiation is uniformly distributed in all horizontal directions, making it ideal for applications that require broad and uniform coverage, such as mobile communication base stations or general broadcasting.

The omnidirectional nature ensures that signals are transmitted and received equally well from all directions, facilitating seamless connectivity for devices within the coverage area.

Mode-2 - Horizontal Polarization with Broadside Radiation

Figure 12 (b) shows the radiation pattern for Mode-2, where the antenna demonstrates horizontal polarization with broadside radiation. This pattern is achieved through the Vivaldi antenna component, known for its highly directional coverage. The broadside radiation pattern indicates that the antenna radiates most strongly in the direction perpendicular to its plane.

This makes Mode-2 suitable for point-to-point communication links, radar systems, or high-frequency data transmission scenarios where focused and directed energy is essential for maintaining strong signal integrity over specific paths.

Mode-3 - Left-Tilted Radiation Pattern

In Figure 12 (c), the radiation pattern corresponds to Mode-3, which features a 90° phase difference between the ports. This phase difference causes constructive and destructive interference between the two symmetrical Vivaldi antennas, resulting in a left-tilted radiation pattern. The enhanced radiation on the left side and suppressed radiation on the right indicate the antenna's ability to steer the beam through phase control.

This directional control is beneficial for applications requiring targeted coverage or interference mitigation in specific directions, enhancing the antenna's adaptability in dynamic environments.

Mode 4 - Right-Tilted Radiation Pattern

Figure 12 (d) illustrates the radiation pattern for Mode-4, characterized by a -90° phase difference between the ports. Similar to Mode 3, the phase difference leads to constructive and destructive interference, but in this case, the pattern is right-tilted. The currents and electric fields superimpose on the right side and cancel out on the left, demonstrating the antenna's beam steering capability.

This mode is particularly useful for applications where directional flexibility is needed, allowing the antenna to dynamically adjust its radiation pattern to optimize coverage and reduce interference.

These varying radiation patterns across the four modes highlight the antenna's versatility in adapting its radiation characteristics through phase control. This feature is crucial for advanced wireless communication systems, including 5G, where different radiation patterns and polarizations can be leveraged to optimize coverage, capacity, and overall network performance. The ability to switch between omnidirectional, directional, and tilted patterns allows the UWB Share-Aperture Antenna to meet the diverse requirements of modern communication environments effectively.

5.1.3 Current Distribution

"Current distribution" refers to the way electric current varies along the length of the antenna element(s). This distribution is crucial in determining the antenna's radiation pattern, impedance, and overall performance.

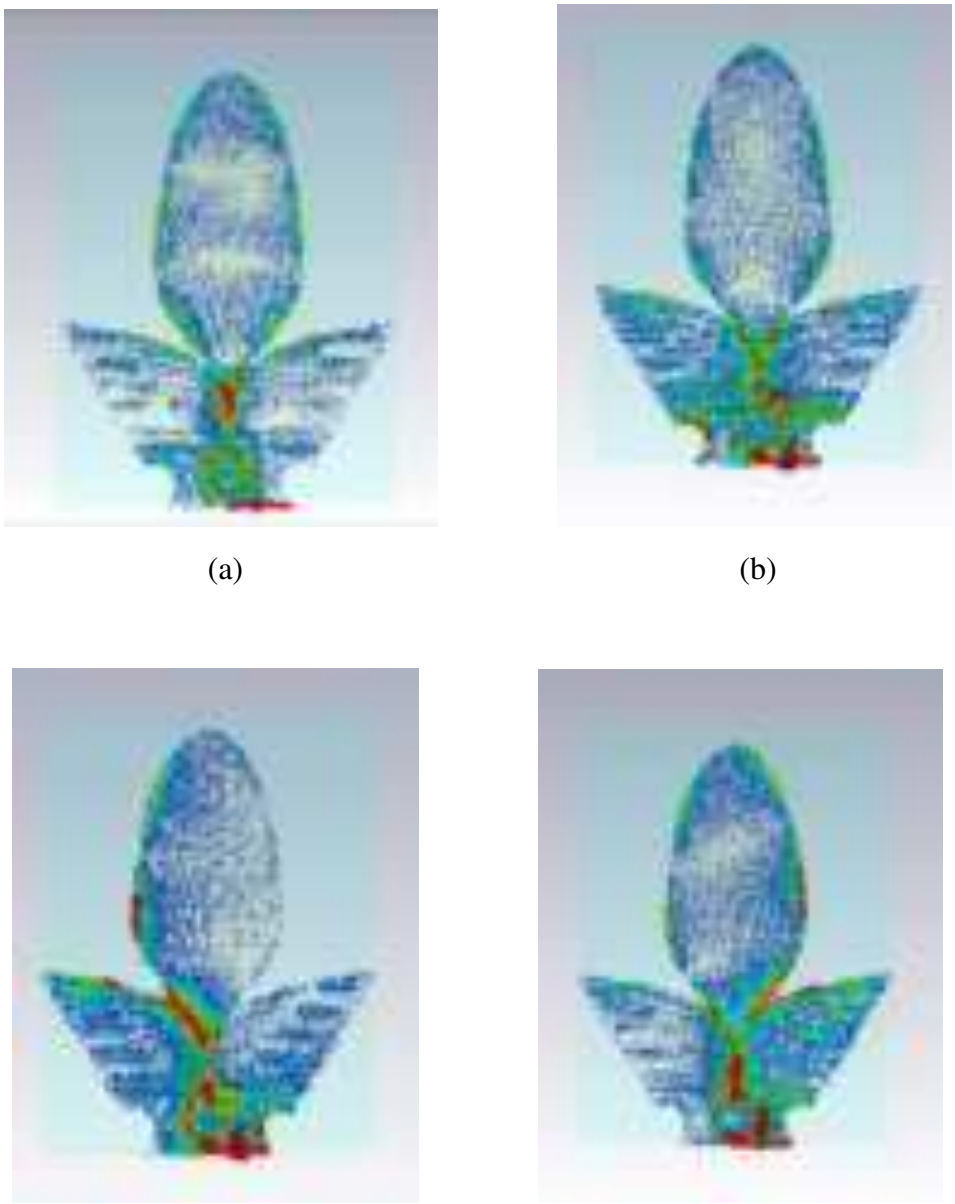

(a) (b)

(c) (d)

Fig. 13 Simulated Result - Current Distribution (a) Mode-1 (b) Mode-2 (c) Mode-3 (d) Mode-4

The radiation pattern of an antenna is directly influenced by its current distribution. Constructive and destructive interference of the electromagnetic waves, produced by different segments of the antenna, shape the final radiation pattern. For example, in a half-wave dipole antenna, the current distribution leads to a broadside radiation pattern, with the maximum radiation occurring perpendicular to the length of the dipole.

The input impedance of the antenna is also affected by the current distribution. At resonance, the impedance has a real component with minimal reactive component, optimizing power transfer. The impedance varies along the length of the antenna, corresponding to the voltage and current standing waves.

The current distribution in an antenna is a critical factor that influences its radiation pattern, efficiency, and overall performance. The provided image shows the current distribution for four different modes (1-4) of the Ultra-Wideband (UWB) share-aperture antenna designed for 5G sub-6 GHz applications.

Each mode reveals unique characteristics, emphasizing the antenna's versatility and adaptability across different operating frequencies.

Mode-1: Concentrated Current Distribution at the Lower Part

In Mode-1 i.e. Fig. 13(a), the current distribution at freq 4.8 GHz is concentrated primarily at the lower part of the antenna structure. This indicates a strong resonance in this region, which is likely associated with a specific frequency band within the UWB range.

The concentration of current suggests that the antenna is effectively tuned to radiate efficiently at this lower frequency. This mode is particularly advantageous for applications requiring robust performance at lower sub-6 GHz frequencies, such as initial 5G deployment phases or legacy LTE support, where strong and reliable signal transmission is crucial.

Mode-2: Uniform Current Distribution Across the Surface

In Mode-2 i.e. Fig. 13(b) shows a more uniform current distribution at freq 5.288 GHz across the entire surface of the antenna . This uniformity suggests efficient radiation and minimal hotspots, indicating that the antenna is operating effectively at a different frequency band.

The even distribution of current is beneficial for achieving a consistent radiation pattern and improving overall antenna efficiency. This mode is ideal for mid-band 5G applications, where balanced performance across a broad range of frequencies is essential to support high data rates and reliable communication over varying distances.

Mode-3: Current Concentration Towards the Edges

In Mode-3 i.e. Fig. 13(c), the current distribution at freq GHz is concentrated towards the edges of the antenna structure. This pattern indicates a distinct radiation characteristic and likely corresponds to another resonance frequency within the UWB spectrum.

The edge concentration may result in a more directional radiation pattern, which can be useful for applications requiring focused energy transmission, such as targeted high-speed data links or specific directional communication channels. This mode's unique distribution enhances the antenna's ability to adapt to specific frequency bands where edge-driven resonance is beneficial.

Mode-4: Balanced Current Distribution

In Mode-4 i.e. Fig. 13(d) demonstrates a balanced current distribution throughout the antenna at freq 5 GHz. This balanced pattern suggests an optimized performance for yet another frequency band, providing a harmonious radiation characteristic that can cater to diverse communication needs.

The balanced distribution is particularly useful for applications demanding consistent performance across multiple frequency bands, ensuring that the antenna can seamlessly support various 5G sub-6 GHz requirements. This mode enhances the antenna's versatility, making it suitable for complex communication environments where different frequencies are used concurrently.

5.1.4 Cross Polarization

Cross-polarization is an important characteristic in antenna systems, representing the component of the electromagnetic wave that is polarized orthogonally to the intended polarization. Understanding cross-polarization in various antenna modes is crucial for optimizing performance and minimizing unwanted interference. Here, we examine the cross-polarization characteristics of four different antenna modes in detail.

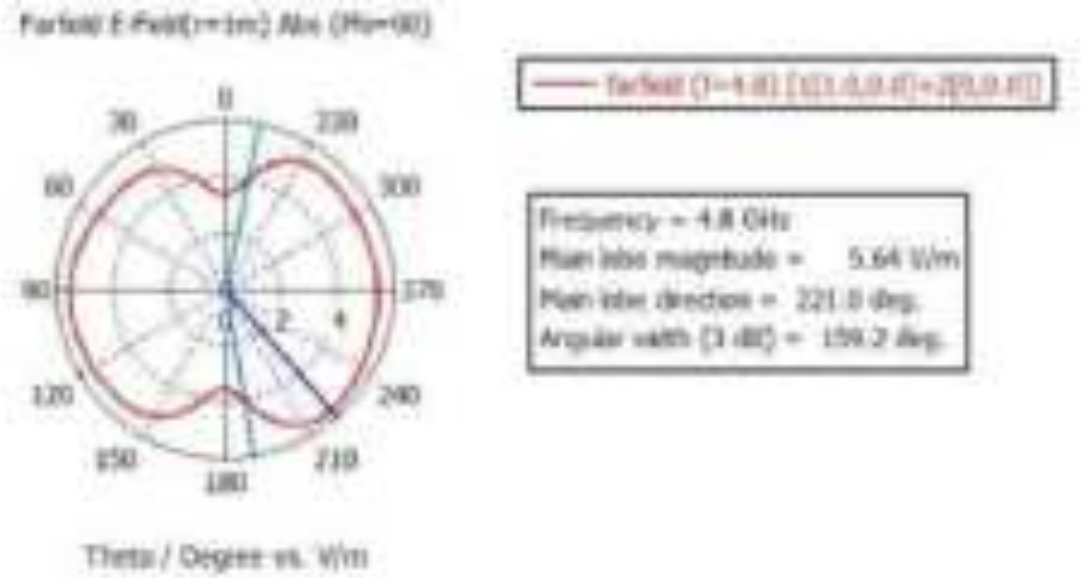

(a)

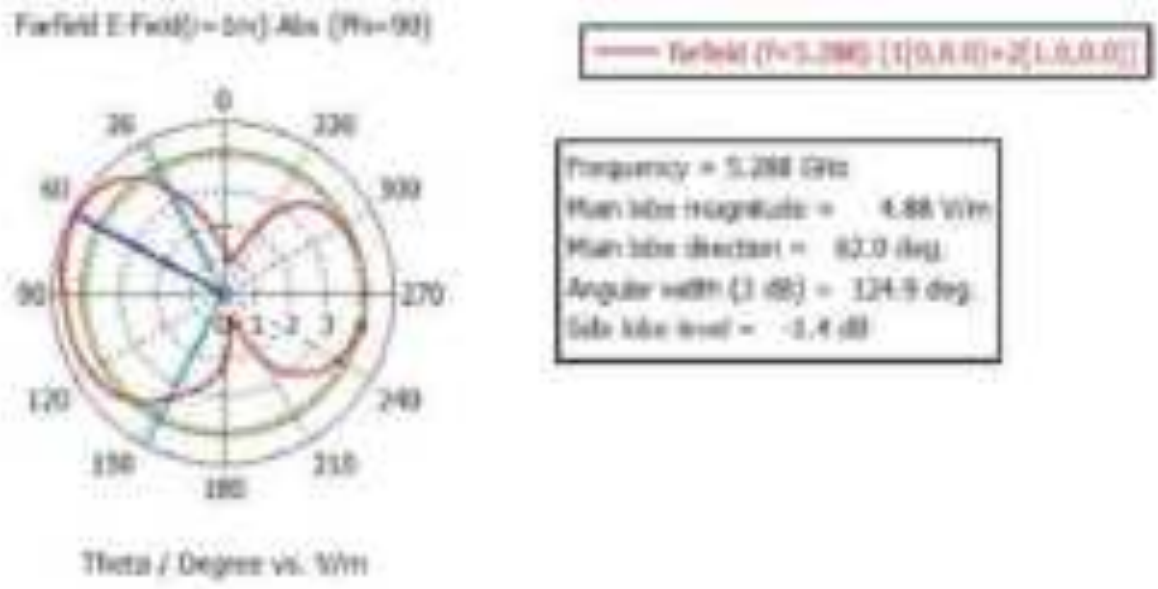

(b)

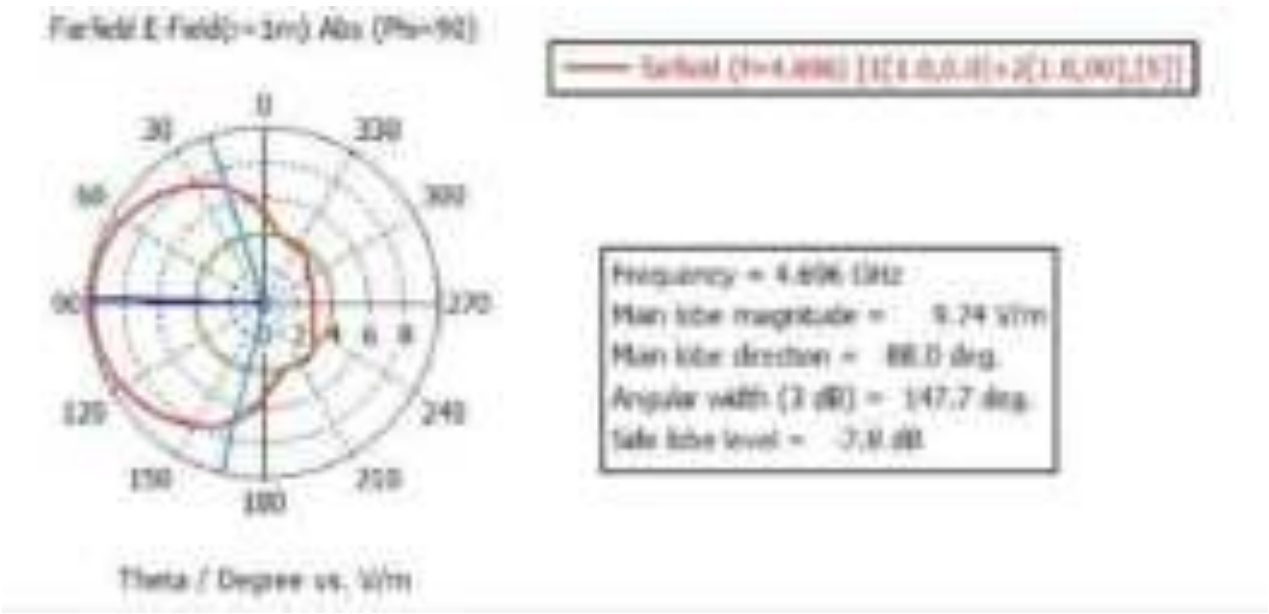

(c)

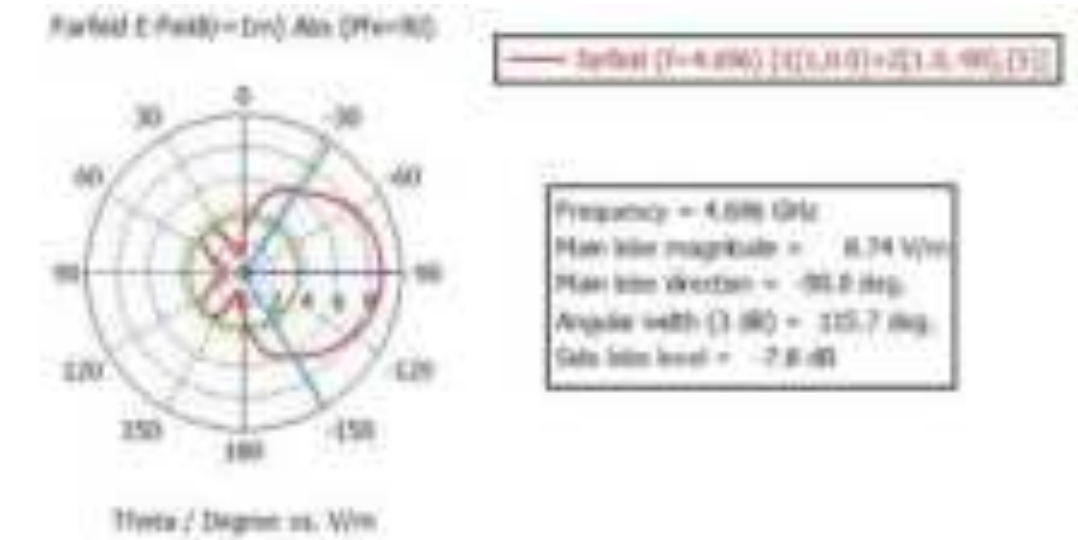

(d)

Fig 14 Simulated Result - Cross Polarization (a) Mode-1 (b) Mode-2 (c) Mode-3

(d) Mode-4

Mode-1 i.e. Fig. 14(a) displays a main lobe magnitude of 5.64 V/m, with the direction of the main lobe at 221.0 deg. and an angular width of 159.2 deg.. This mode reflects the behavior of a monopole antenna, known for its omnidirectional radiation pattern.

The broad angular range indicates that the cross-polarization is widely distributed, lacking a specific directional focus. This widespread cross-polarization is typical for monopole antennas, which are often used in applications requiring coverage over a large area, although it may lead to higher susceptibility to interference from unwanted directions.

Mode-2 i.e. Fig. 14(b) with a main lobe magnitude of 4.88 V/m, points its main lobe at 62.0 deg. and has an angular width of 124.9 deg.. Additionally, it exhibits a side lobe level of -1.4 dB.

This mode is characteristic of the Vivaldi antenna, which is known for its directional properties. The cross-polarization in this mode is more concentrated in a specific direction compared to Mode-1, indicating that the Vivaldi antenna can better control the distribution of cross-polarized energy. This focused cross-polarization is advantageous in applications requiring precise targeting and minimal interference from adjacent directions.

Mode-3 i.e. Fig. 14(c) presents a main lobe magnitude of 9.74 V/m, with the main lobe directed at 88.0 deg. and an angular width of 147.7 deg.. The side lobe level is recorded at -7.8 dB. This mode shows a substantial increase in the main lobe magnitude, suggesting stronger cross-polarization.

Despite being more directional than Mode-1, the broad pattern of Mode-3 indicates that the cross-polarized energy is still somewhat widespread. The higher main lobe magnitude and significant side lobe suppression suggest that this mode is more suitable for applications where a balance between directionality and coverage is needed, providing robust performance in scenarios with potential cross-polarization interference.

Mode-4 i.e. Fig. 15(c) features a main lobe magnitude of 8.74 V/m, with the main lobe direction at -90.0 deg. and an angular width of 115.7 deg.. It also has a side lobe level of -7.8 dB. Similar to Mode-3, Mode-4 shows a strong and directional cross-polarization pattern but with a slightly narrower angular width.

This indicates that the cross-polarized energy is more focused, providing a higher degree of control over the orthogonal polarization direction. The combination of a strong main lobe and effective side lobe suppression makes this mode ideal for applications requiring precise and concentrated cross-polarization management, ensuring better performance in environments with high interference potential.

4.1.5 Co-Polar Representation

Co-polarization refers to the component of the radiated electromagnetic field that aligns with the intended polarization of the antenna. This is the desired orientation of the electric field vector of the radiated waves, which can be linear (horizontal or vertical), circular (right-hand or left-hand), or elliptical. When analysing an antenna's performance, the co-polarized component is crucial as it indicates how well the antenna transmits or receives signals with the intended polarization.

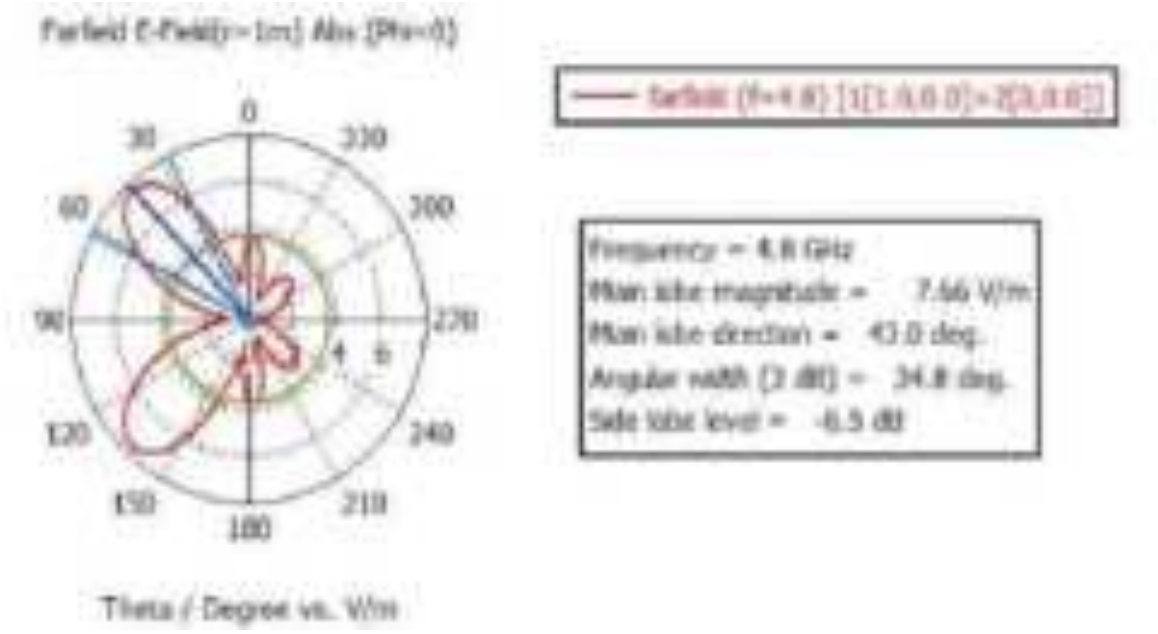

Fig. 15 (a) Simulated Result - Co-Polarization - Mode-1

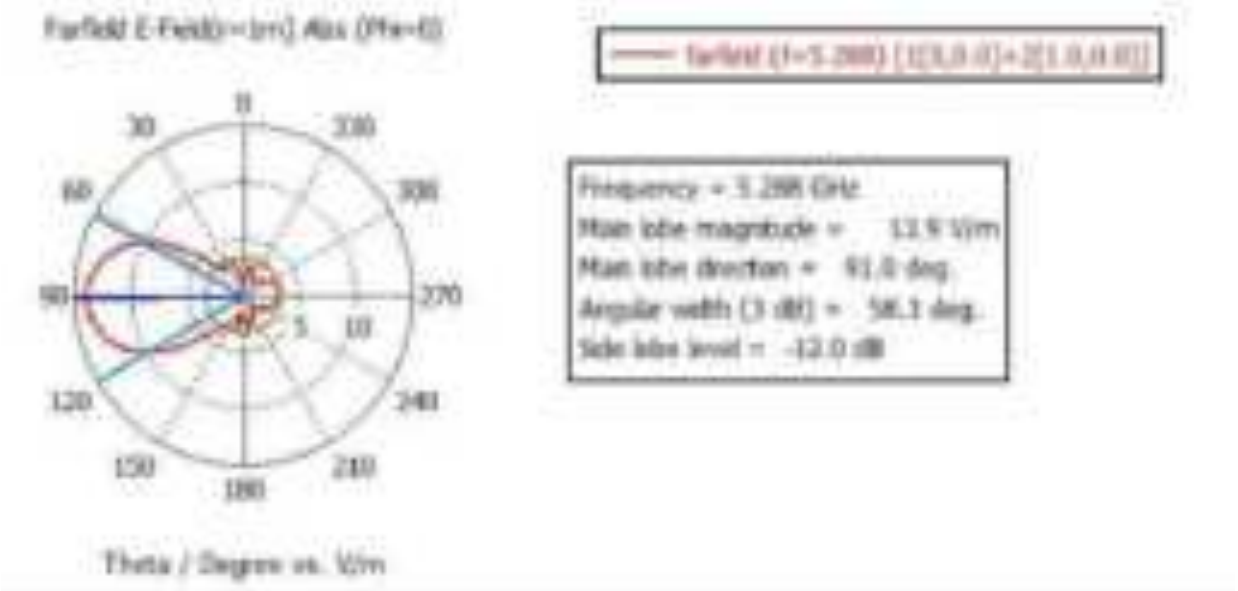

Fig. 15 (b) Simulated Result - Co-Polarization - Mode-2

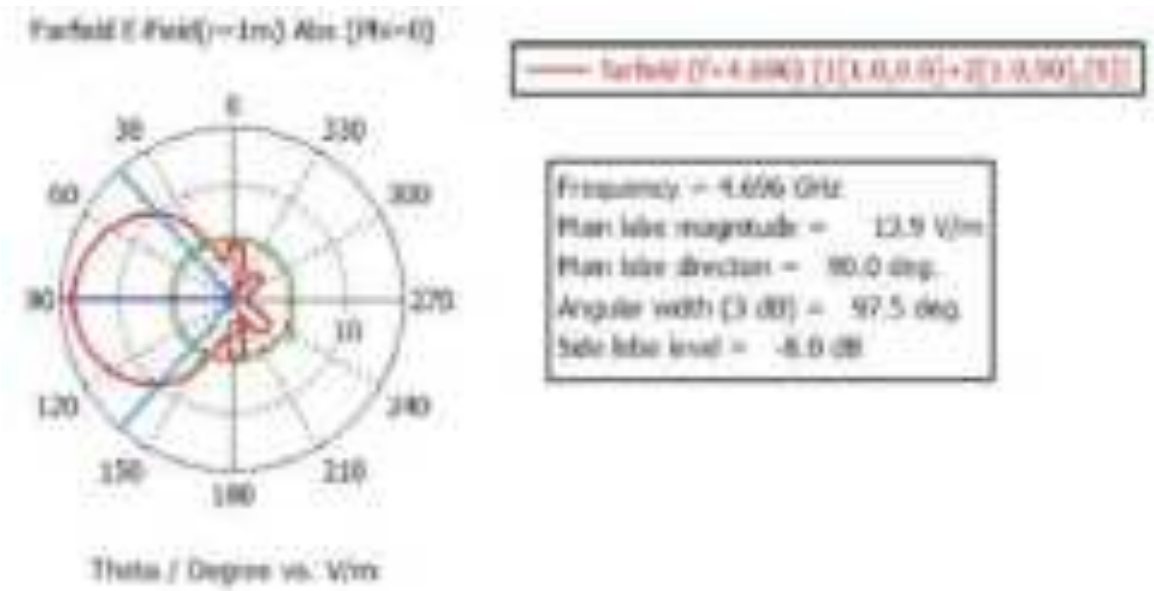

Fig. 15 (c) Simulated Result - Co-Polarization Mode-3

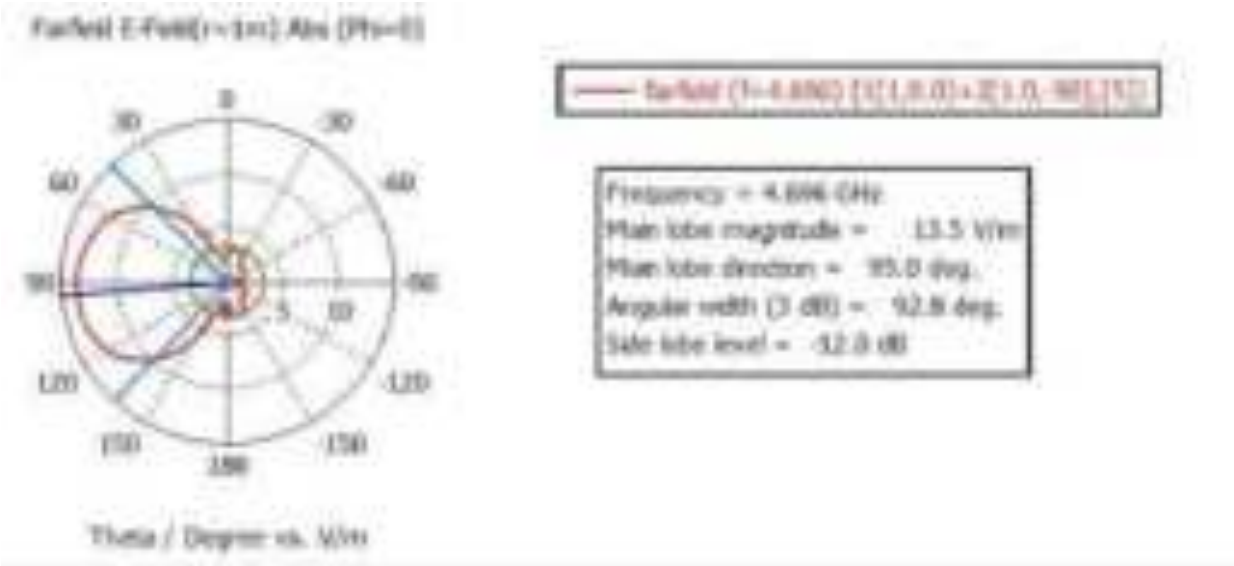

Fig. 15 (d) Simulated Result - Co-Polarization - Mode-4

Mode-1 i.e. Fig. 15(a)showcases a co-polarization main lobe magnitude of 7.66 V, directed at 43 deg.. The angular width of 34.8 deg. is the narrowest among the modes, highlighting the focused nature of the antenna's radiation pattern in this configuration.

The side lobe level of -6.5 dB indicates a moderate level of side lobe suppression. This mode is indicative of an antenna setup designed for applications requiring a highly directional signal with minimal spread, providing a concentrated beam that is beneficial for point-to-point communication systems where reducing interference is crucial.

Mode-2 i.e. Fig. 15(b) stands out with the highest main lobe magnitude of 13.9 V, directed at 91 deg.. Operating at a frequency of 5.288 GHz, this mode has an angular width of 58.3 deg.. The side lobe level of -12 dB signifies a significant improvement in side lobe suppression compared to Mode-1, which suggests enhanced performance in minimizing interference from directions outside the main beam.

The higher main lobe magnitude and better side lobe suppression make this mode particularly suitable for applications that demand high signal strength and clarity, such as high-frequency data transmission or precise radar systems.

Mode-3 i.e. Fig. 15(c) features a main lobe magnitude of 5.28 dBi, with the direction fixed at 90 deg.. The angular width of 97.5 deg. is quite broad, indicating a wider spread of the co-polarized signal. The side lobe level of -8.0 dB provides a moderate level of suppression, balancing between maintaining a strong main lobe and managing side lobes.

This mode is suitable for applications requiring a wider coverage area with a reasonable level of directivity and control over side lobes, making it ideal for broadcast applications or general-purpose communications where both range and coverage are important.

Mode-4 i.e. Fig. 15(d) has a main lobe magnitude of 3.19 V, directed at 95 deg.. The angular width is 83.7 deg., measured at the 3 dB points, indicating a moderately wide beam. The side lobe level of -13.6 dB is the lowest among the modes, suggesting excellent side lobe suppression.

This characteristic makes Mode-4 highly effective for applications that require precise directivity and minimal interference from unwanted directions, such as in highly cluttered environments or in applications where adjacent channel interference must be minimized. The combination of good directivity and low side lobe levels makes this mode ideal for scenarios where signal purity and focus are paramount.

5.1.6 FarField Gain

The far-field gain of an antenna is a critical parameter that determines its effectiveness in various communication scenarios. Each of the four operational modes of the antenna demonstrates distinct radiation characteristics, making them suitable for different 5G Sub-6G applications. Here's a detailed analysis of each mode:

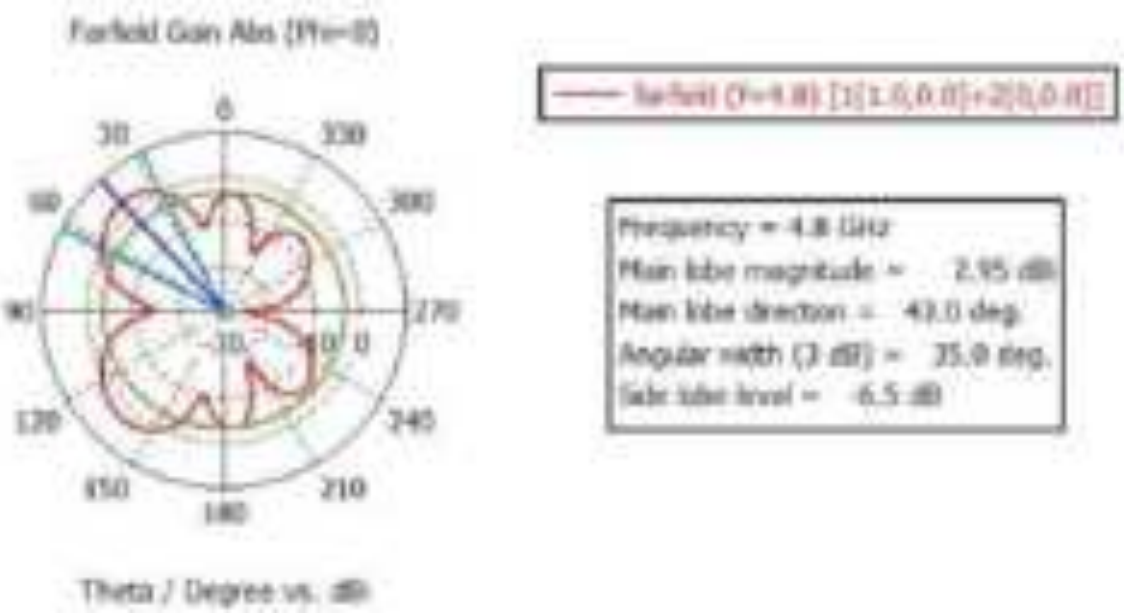

Fig. 16 (a) Simulated Result - FarField Gain - Mode-1

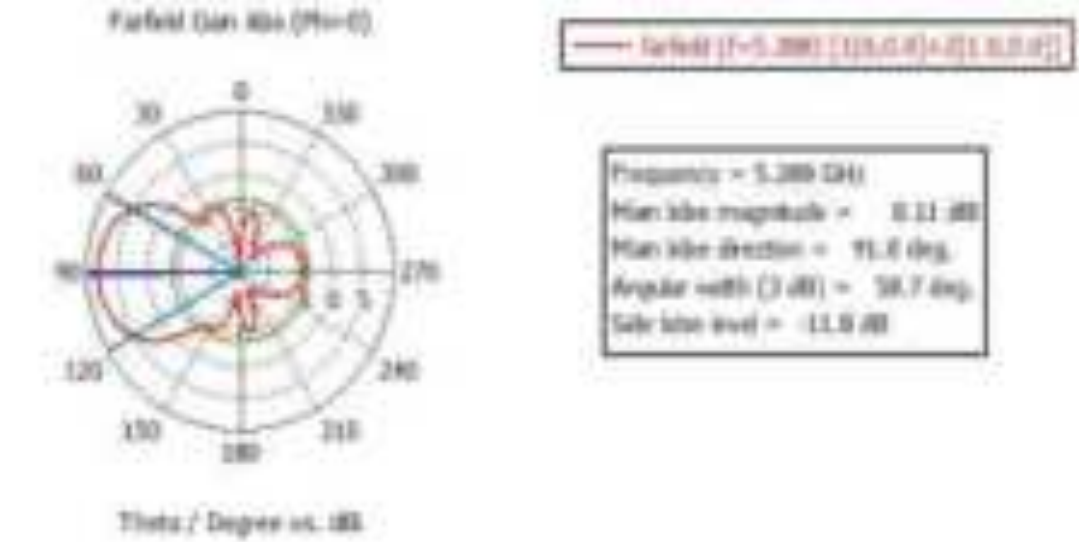

Fig. 16 (b) Simulated Result - FarField Gain - Mode-2

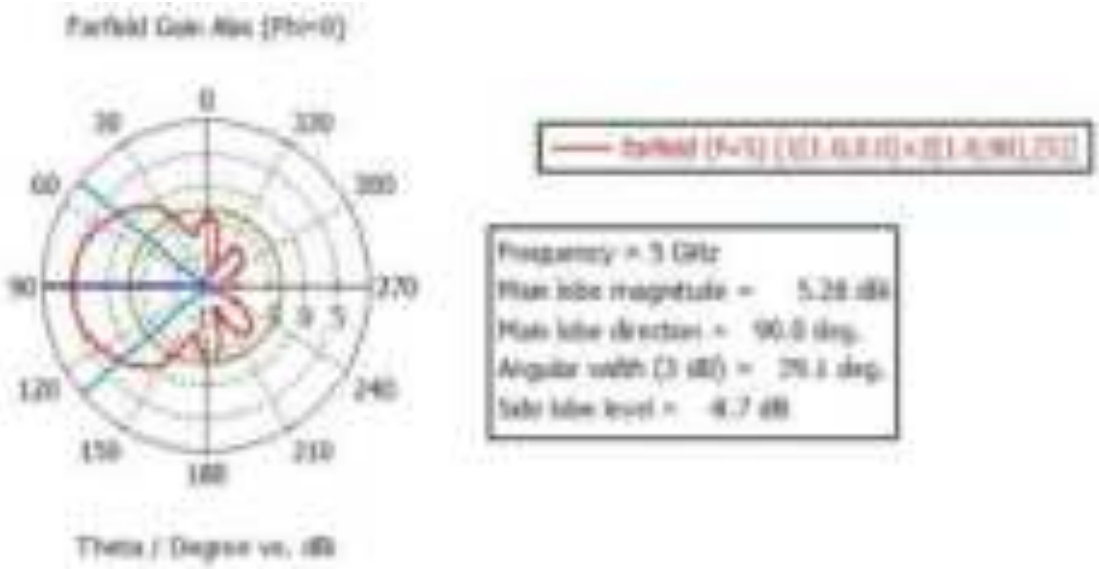

Fig. 16 (c) Simulated Result - FarField Gain - Mode-3

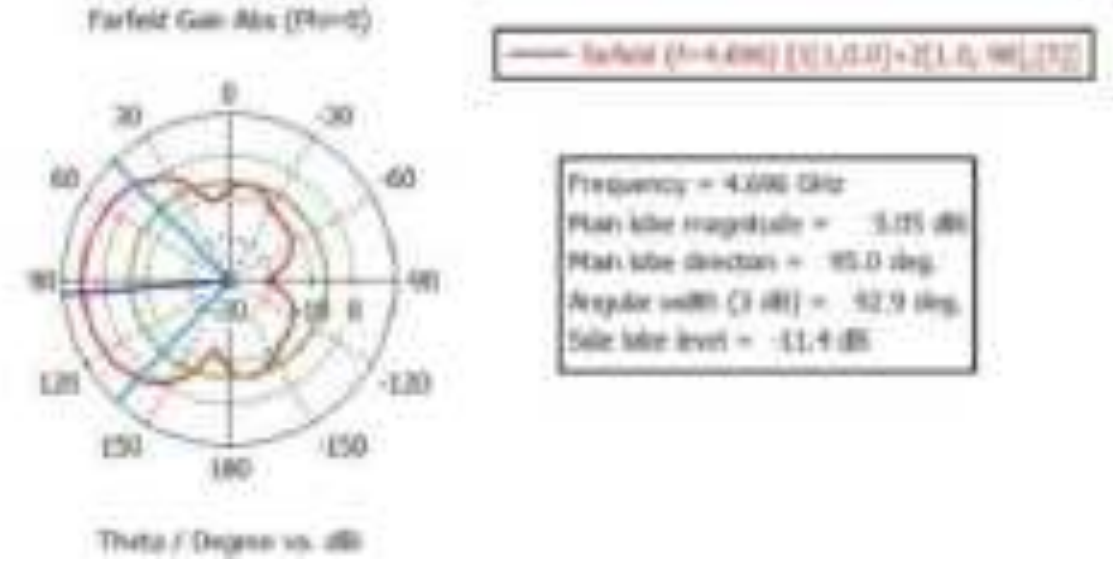

Fig. 16 (d) Simulated Result - FarField Gain - Mode-4

Mode-1: Omnidirectional Radiation Pattern

Fig. 16(a) exhibits an omnidirectional radiation pattern, which is characteristic of monopole antennas. It has a gain of 2.95 dBi at an angle of 43 deg.. The angular width is relatively narrow at 35 deg., and the side lobe level is -6.5 dB. This configuration is particularly well-suited for applications that require uniform coverage in all directions, such as in mobile communication base stations or for general broadcast applications.

The moderate side lobe suppression indicates that while the antenna can provide widespread coverage, there is some potential for interference from side lobes, which may need to be managed depending on the specific application environment.

Mode-2: Highly Directional Vivaldi Antenna Characteristics

Fig. 16(b) showcases the properties of a Vivaldi antenna, which is known for its high directionality. It achieves a substantial gain of 8.11 dBi at 91 deg. with an angular width of 58.7 deg.. The side lobe level is significantly lower at -11.8 dB, highlighting its effectiveness in minimizing interference from unwanted directions.

This makes Mode-2 ideal for scenarios requiring focused energy transmission, such as point-to-point communication links, radar systems, or high-speed data transmission in densely populated urban environments where directed beams are necessary to avoid interference and ensure signal integrity.

Mode-3: Balanced Gain and Angular Width

Fig. 16(c) provides a balanced performance between gain and angular width. It has a gain of 5.28 dBi at 90 deg. and an angular width of 79.1 deg., offering a broader beam compared to Mode-2 but with slightly reduced gain. The side lobe level is -8.7 dB, which indicates good suppression of side lobes.

This mode is suitable for applications requiring a wide coverage area with moderate gain, such as suburban cellular networks or wide-area wireless communications where a balance between range and coverage is necessary. The broader beam ensures that a larger area is covered, making it effective for scenarios where users are spread out over a wide region.

Mode-4: Extensive Coverage with Excellent Side Lobe Suppression

Fig. 16(d), similar to Mode-3, has a gain of 5.05 dBi but is directed at 95 deg.. It has the broadest angular width at 92.9 deg., making it advantageous for extensive coverage. The side lobe level of -11.4 dB indicates excellent side lobe suppression, which is beneficial in environments where interference reduction is critical.

This mode is ideal for large-scale coverage applications, such as rural broadband networks or extensive indoor environments like large warehouses or shopping malls, where the antenna needs to cover a wide area while minimizing interference from surrounding objects or other communication systems.

5.2 MEASURED RESULT OF ANTENNA

We had perform the fabricated antenna in VNA for the desired results and we got the results we are unable to perform the mode3 and mode4 cause these modes are actually need the fabrication of feeder which we didn't fabricate cause of lack of availability of Taconic TLY5 substrate plate.

Fig17 Results in VNA screen

5.2.1 Description and Analysis of Fig 18 (a):

The Fig. 18 (a) shown is a plot of the S22 parameter (in dB) versus frequency (in Hz) for Mode-2 of an antenna made using monopole and Vivaldi structures. Here's a detailed analysis of the information provided by this graph:

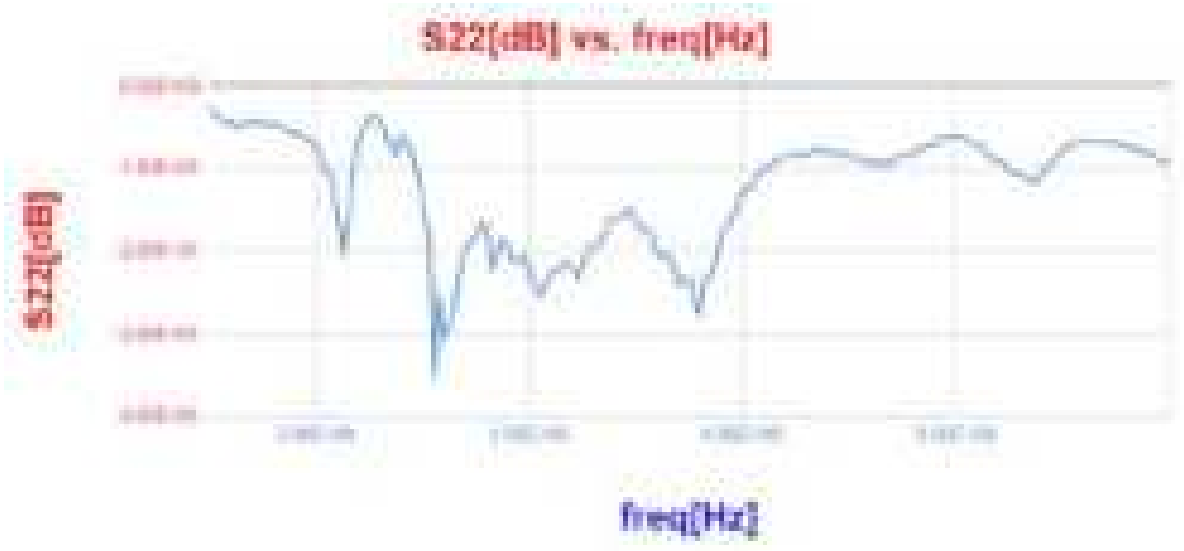

Fig 18(a) Measured s-parameters of Mode-2

1. **Parameter Displayed: S22[dB]** represents the reflection coefficient at Port 2 when Port 2 is active and Port 1 is inactive (Port 1 = 0, Port 2 = 1). **Frequency Range:** The x-axis indicates the frequency range in Hz, with major ticks at 2 GHz, 4 GHz, 6 GHz, and 8 GHz.

2. **Operational Bandwidth:** The operational bandwidth for this mode spans from 1.9 GHz to 5.9 GHz. This means the antenna is designed to perform optimally within this frequency range when Port 2 is active

.**3**. **Performance Characteristics:**

- **Reflection Coefficient (S22):** The graph shows how well the antenna is matched to the transmission line at Port 2. Lower values (in dB) indicate better matching and less reflected power.
- **Notable Features:**
  - **Peaks and Dips:** Significant dips (minima) in the S22 plot correspond to frequencies where the antenna is well-matched, meaning minimal power is reflected back. For example, there is a notable dip around 4 GHz.
  - **Broadband Performance:** The graph suggests a relatively broad performance over the indicated operational bandwidth.

4. Optimization Insights:

The slight narrowing of the bandwidth in this mode could indicate that the antenna is optimized for specific applications within the 1.9 GHz to 5.9 GHz range. This can be beneficial for applications requiring focused performance in narrower frequency bands.

5. Graph Labels and Axes:

Y-Axis (S22[dB]): The left vertical axis, labelled in red, measures the reflection coefficient in decibels. The range shown goes from 0 dB (no reflection) to -40 dB (very low reflection).

X-Axis (Frequency [Hz]): The horizontal axis, labelled in blue, shows the frequency in Hz, indicating a range from 2 GHz to 8 GHz, with the axis scale shown in scientific notation (e.g., 2.00E+09 Hz).

5.2.2 Description and Analysis of Fig 18 (b) :

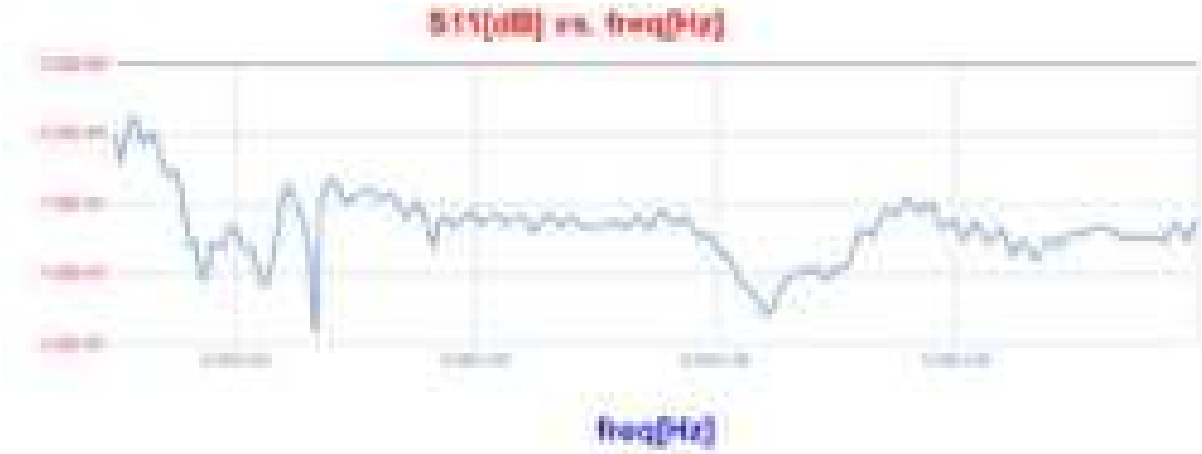

Fig 18(b) Measured s-parameters of mode1

1. **Parameter Displayed: S_{11}[dB]:** This represents the reflection coefficient at Port 1 when Port 1 is active. S_{11} measures how much power is reflected back to the source from Port 1. Lower values (in dB) indicate better impedance matching and less power reflection.
2. **Frequency Range:** The x-axis indicates the frequency range in Hz, with major ticks at 2 GHz, 4 GHz, 6 GHz, and 8 GHz. The scale is displayed in scientific notation (e.g., 2.00E+09 for 2 GHz).
3. **Performance Characteristics:**
    - **Reflection Coefficient (S_{11}):** The graph shows how well the antenna is matched to the transmission line at Port 1. Lower S_{11} values indicate better matching, meaning less reflected power.
    - **Notable Features:**
        - **Peaks and Dips:** Significant dips in the S_{11} plot correspond to frequencies where the antenna is well-matched. For example, there is a notable dip around 2.5 GHz and another one near 6 GHz.
        - **Broadband Performance:** The graph suggests the antenna has reasonable performance over a broad range of frequencies, but the exact operational bandwidth would need to be specified based on acceptable reflection levels (e.g., below -10 dB).

Graph Labels and Axes:

1. **Y-Axis (S_{11} [dB]):** The left vertical axis, labeled in red, measures the reflection coefficient in decibels. The range shown goes from 0 dB (no reflection) to -20 dB (very low reflection). This range helps identify how well the antenna is matched across different frequencies.
2. **X-Axis (Frequency[Hz]):** The horizontal axis, labeled in blue, shows the frequency in Hz. The major ticks at 2 GHz, 4 GHz, 6 GHz, and 8 GHz indicate the span of the frequency range.

Key Takeaways:

- **Impedance Matching:** The antenna shows good matching around the dips in the S11 plot. These frequencies indicate minimal reflection, meaning the antenna is effectively radiating the power.
- **Operational Bandwidth:** The operational bandwidth can be determined by identifying the frequency range where the S11 values are below a certain threshold (e.g., -10 dB), indicating good performance. For Mode-1, based on the plot, the antenna has notable performance dips at around 2.5 GHz and 6 GHz, suggesting effective operation near these frequencies.

5.2.3 Description and Analysis of Fig 18 (c):

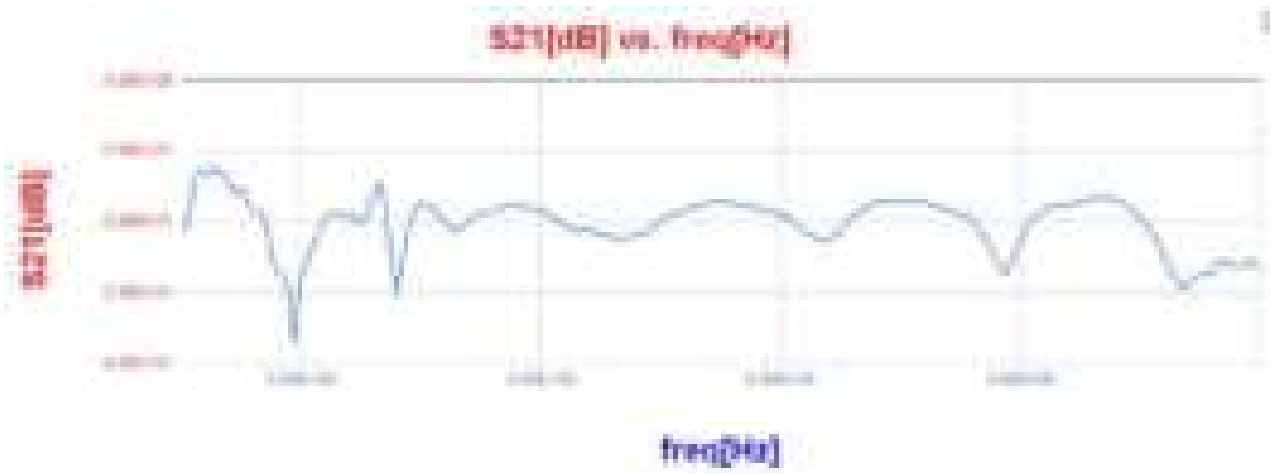

Fig 18(c) Coupling Coefficient of mode-1 and mode-2

1. **Parameter Displayed:** S_{21} **[dB]:** This represents the transmission coefficient from Port 1 to Port 2. It indicates how much power is transferred from one port to the other, which is crucial for understanding the coupling between the ports.
2. **Frequency Range:**The x-axis indicates the frequency range in Hz, with major ticks at 2 GHz, 4 GHz, 6 GHz, and 8 GHz. The scale is displayed in scientific notation (e.g., 2.00E+09 for 2 GHz).
3. **Performance Characteristics:**
    - **Transmission Coefficient** (S_{21})**:** The graph shows how much power is transmitted from Port 1 to Port 2. Higher values indicate better transmission, meaning less power is lost between the ports.
    - **Notable Features:** Significant dips in the S_{21} plot correspond to frequencies where there is poor transmission between the ports. For example, there is a notable dip around 2 GHz and another one around 6 GHz.

Graph Labels and Axes:

1. **Y-Axis (S21[dB]):** The left vertical axis, labeled in red, measures the transmission coefficient in decibels. The range shown goes from 0 dB (no loss) to -40 dB (high loss). This range helps identify how well the antenna transmits power between the ports across different frequencies.
2. **X-Axis (Frequency [Hz]):** The horizontal axis, labeled in blue, shows the frequency in Hz. The major ticks at 2 GHz, 4 GHz, 6 GHz, and 8 GHz indicate the span of the frequency range.

Key Takeaways:

1. **Coupling Between Ports:**The S21 parameter provides insights into the efficiency of power transfer between Port 1 and Port 2. Lower S_{21} values indicate more loss, whereas higher values indicate better coupling and power transfer.
2. **Operational Bandwidth:** The operational bandwidth can be determined by identifying the frequency range where the S21 values are above a certain threshold (e.g., -20 dB), indicating acceptable power transfer levels.
3. **Application Optimization:**Depending on the specific application requirements, the antenna can be optimized further to ensure the desired frequencies have the highest possible S21 values for minimal loss and maximum power transfer.

5.3 SIMULATED RESULT OF FEEDER

5.3.1 S-Parameter

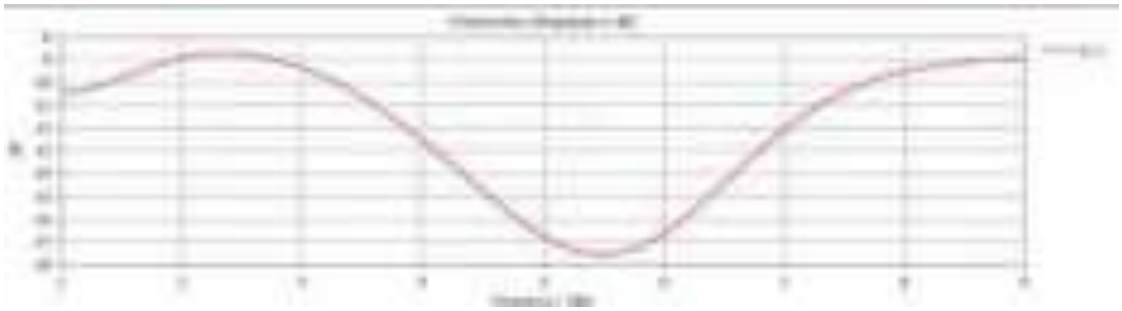

Fig. 19 Simulated S-parameter of feeder (S_{11})

In Fig 19 shows S- Parameter S11 in decibels (dB) versus frequency in GHz.overs a frequency range from 1 GHz to 9 GHz. where the y-axis represents the magnitude of S11 in dB, ranging from -18 dB to -8 dB.

Observations:

At low frequencies around 2 GHz, the S11 parameter exhibits a peak with a value of approximately -9 dB. As the frequency increases, the S11 magnitude decreases, reaching a minimum value of around -17 dB near 5.5 GHz, indicating better impedance matching and reduced reflection at this frequency.

At higher frequencies, as the frequency approaches 9 GHz, the S11 magnitude increases again, returning to approximately -9 dB. This behavior suggests that the antenna has varying impedance matching characteristics across the frequency spectrum, with optimal performance near the mid-frequency range around 5.5 GHz.

Interpretation:

- **Return Loss:** S_{11} parameter represents the return loss or the reflection coefficient of the system. Lower values of S_{11} (more negative) indicate better impedance matching and less reflection.
- **Resonance:** The dip around 5.5 GHz suggests a resonant frequency where the impedance matching is optimal, leading to minimal reflection.
- **Performance:** The system appears to perform best around 5.5 GHz, as indicated by the lowest S11 value.

5.3.2 Current Distribution

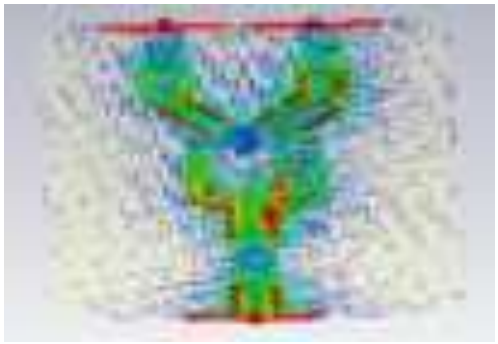

Fig. 20 Current distribution of feeder at 5GHz

The Fig. 20 shows a simulation of the surface current distribution on a structure at a frequency of 5 GHz and a phase of 90 degrees, the surface current distribution on the antenna structure is observed.

The maximum current density reaches 16 A/m. The color bar on the right indicates the range of current density values from 0 to 16 A/m, with colors representing the magnitude of the surface current density. Red areas indicate the highest current density, while blue areas indicate the lowest. The structure shows areas of high current density (in red) near the top and bottom sections and around the central part. The coordinate system is displayed with the x, y, and z axes for reference.

Interpretation:

- **Current Concentration:** The high current density areas (in red) suggest where the current is concentrated on the structure at this specific frequency and phase.
- **Design Implications:** These areas might correspond to critical points in the design, such as feeding points, resonant sections, or areas where the current is expected to be high due to the structure's geometry or the nature of the excitation.

CHAPTER 6 CONCLUSION

6.1 OUTCOME OF STUDY

In this research, we successfully designed and fabricated a broadband antenna utilizing CST 2019 for simulation and manual fabrication techniques in the lab. The antenna design featured a copper patch on an FR4 lossy substrate, created through a precise masking process.

Our fabricated antenna exhibited a wide operational bandwidth ranging from 1.17 GHz to 7 GHz, demonstrating its suitability for broadband applications. Notably, the antenna achieved a commendable gain of 8.11 dBi, indicative of its efficiency in directing radiated power.

The performance metrics were further substantiated by a bandwidth gain percentage of 142.72%, underscoring the antenna's effectiveness across its broad frequency range. This high bandwidth gain percentage highlights the antenna's capability to maintain robust performance over a substantial portion of its operational spectrum.

Our comparative analysis between the simulated and measured results validated the design methodology, emphasizing the importance of detailed simulations in predicting real-world performance. The surface current distribution analysis at 5 GHz provided critical insights into the areas of high current concentration, which informed the design refinements and contributed to the overall success of the fabricated antenna.

6.2 FUTURE SCOPE

For future work, several avenues can be explored to enhance the performance and applicability of the designed antenna:

6.2.1 Integration with Wilkinson Power Divider:

The initial CST simulation of a stage 1 Wilkinson power divider as a feeder for the designed antenna shows promising results with S11<−10 dB and a gain of 7.2 dBi. Further development and integration of this power divider can improve the feeding network's efficiency and the antenna's overall performance.

6.2.2 Multi-port Excitation:

Investigating the performance of the antenna with both discrete port excitation and waveguide port excitation for monopole and Vivaldi antennas can provide deeper insights into the optimal feeding methods and enhance radiation characteristics.

6.2.3 Advanced Material Exploration:

While FR4 was used for this design, exploring substrates with lower dielectric loss and higher thermal stability could lead to improved performance, especially at higher frequencies.

6.2.4 Array Configurations:

Developing antenna arrays using the designed element can significantly enhance gain and directivity. This would involve studying the mutual coupling effects and optimizing the array layout for specific applications.

6.2.5 Miniaturization and Compact Design:

Efforts can be made to miniaturize the antenna design while maintaining its wide bandwidth and high gain, making it suitable for compact and portable wireless devices.

6.2.6 Environmental Testing:

Extensive testing in different environmental conditions, such as varying temperatures, humidity levels, and physical obstructions, can provide a comprehensive understanding of the antenna's real-world performance and robustness.

6.2.7 Application-specific Optimization:

Tailoring the antenna design for specific applications, such as 5G communications, Internet of Things (IoT) devices, or vehicular communication systems, can further enhance its utility and performance.

6.2.8 Simulation and Fabrication Refinements:

Continuous refinement of simulation models and fabrication techniques can help in achieving even closer alignment between simulated and measured results, leading to more predictable and reliable antenna designs.

6.2.9 Multi-mode Generation and Beam Steering:

By incorporating a Wilkinson power divider and applying phase shifts, it is possible to generate multiple radiation modes. This approach allows for beam steering capabilities, including left tilt and right tilt of the antenna radiation pattern. Such features can be highly advantageous in dynamic and adaptive communication systems, enabling better control over the radiation direction and improving signal quality in varying conditions.

By pursuing these future directions, the potential of the designed antenna can be fully realized, leading to advancements in broadband communication technologies and various practical applications.

REFERENCES

[1] Y. Cao, S. Yan, J. Li, and J. Chen, "A pillbox based dual circularly-polarized millimeter-wave multi-beam antenna for future vehicular radar applications," IEEE Trans. Veh. Technol., vol. 71, no. 7, pp. 7095–7103, Jul. 2022, doi: 10.1109/TVT.2022.3162299.

[2] Y. Cao, G. A. E. Vandenbosch, and S. Yan, "Low-profile dual-polarized multi-beam antenna based on pillbox reflector and 3D-printed ridged waveguide," IEEE Trans. Antennas Propag., vol. 70, no. 9, pp. 7578–7591, Sep. 2022, doi: 10.1109/TAP.2022.3171728.

[3] L.-K. Zhang, Y.-X. Wang, J.-Y. Li, Y. Feng, and W. Zhang, "Cavitybacked circularly polarized cross-dipole phased arrays," IEEE Antennas Wireless Propag. Lett., vol. 20, no. 9, pp. 1656–1660, Sep. 2021.

[4] S. Shi et al., "Wideband planar phased array antenna based on artificial magnetic conductor surface," IEEE Trans. Circuits Syst. II, Exp. Briefs, vol. 67, no. 10, pp. 1909–1913, Oct. 2020.

[5] M. Noferesti and T. Djerafi, "Controllable orthogonal mode rejection for smart polarization diversity at millimeter-wave frequency," IEEE Trans. Circuits Syst. II, Exp. Briefs, vol. 68, no. 1, pp. 171–175, Jan. 2021.

[6] J. Liu, J.-Y. Li, R. Xu, and S.-G. Zhou, "A reconfigurable printed antenna with frequency and polarization diversity based on bow-tie dipole structure," IEEE Trans. Antennas Propag., vol. 67, no. 12,pp. 7628–7632, Dec. 2019.

[7] R. Xu, J.-Y. Li, J. Liu, S.-G. Zhou, Z.-J. Xing, and K. Wei, "A design of dual-wideband planar printed antenna for circular polarization diversity by combining slot and monopole modes," IEEE Trans. Antennas Propag., vol. 66, no. 8, pp. 4326–4331, Aug. 2018.

[8] L. Li, X. Yan, H. C. Zhang, and Q. Wang, "Polarization-and frequency reconfigurable

patch antenna using gravity-controlled liquid metal," IEEE Trans. Circuits Syst. II, Exp. Briefs, vol. 69, no. 3, pp. 1029–1033, Mar. 2022.

[9] B. Peng, S. Li, J. Zhu, L. Deng, and Y. Gao, "A compact wideband dual-polarized

slot antenna with five resonances," IEEE Antennas Wireless Propag. Lett., vol. 16, pp. 2366–2369, 2017.

[10] A.-N. Nguyen et al., "Dual-polarized slot antenna for full-duplex systems with high isolation," IEEE Trans. Antennas Propag., vol. 69, no. 11, pp. 7119–7124, Nov. 2021.

[11] X. Yang, J. Hu, Y. Ji, L. Ge, and X. Zeng, "Design of a metasurface antenna with pattern diversity," IEEE Antennas Wireless Propag. Lett., vol. 19, no. 12, pp. 2467–2471, Dec. 2020.

[12] S. X. Ta, N. Nguyen-Trong, V. C. Nguyen, K. K. Nguyen, and C. Dao-Ngoc, "Broadband dual-polarized antenna using metasurface for full-duplex applications," IEEE Antennas Wireless Propag. Lett., vol. 20, no. 2, pp. 254–258, Feb. 2021.

[13] C. Deng, X. Lv, and Z. Feng, “Wideband dual-mode patch antenna with compact CPW feeding network for pattern diversity application,” IEEE Trans. Antennas Propag., vol. 66, no. 5, pp. 2628–2633, May 2018.
[14] Y. Zheng and S. Yan, “A low-profile half-mode annular microstrip antenna with pattern diversity,” IEEE Antennas Wireless Propag. Lett., vol. 19, no. 10, pp. 1739–1743, Oct. 2020.

[15] H. Deng, L. Zhu, N.-W. Liu, and Z.-X. Liu, “Single-layer dualmode microstrip antenna with no feeding network for pattern diversity application,” IEEE Antennas Wireless Propag. Lett., vol. 19, no. 12, pp. 2442–2446, Dec. 2020.

[16] P.-Y. Qin, Y. J. Guo, and C. Ding, “A beam switching quasi-yagi dipole antenna,” IEEE Trans. Antennas Propag., vol. 61, no. 10,pp. 4891–4899, Oct. 2013.

[17] W. Zhang, Y. Li, Z. Zhang, and Z. Feng, “A pattern-reconfigurable aircraft antenna with low wind drag,” IEEE Trans. Antennas Propag., vol. 68, no. 6, pp. 4397–4405, Jun. 2020.

[18] W. Wang, Y. Wu, W. Wang, and Y. Yang, “Isolation enhancement in dual-band monopole antenna for 5G applications,” IEEE Trans. Circuits Syst. II, Exp. Briefs, vol. 68, no. 6, pp. 1867–1871, Jun. 2021.

[19] A. Pal, A. Mehta, D. Mirshekar-Syahkal, and H. Nakano, “A twelvebeam steering low-profile patch antenna with shorting vias for vehicular applications,” IEEE Trans. Antennas Propag., vol. 65, no. 8, pp. 3905–3912, Aug. 2017.

[20] N. Hussain and N. Kim, “Integrated microwave and mm-Wave MIMO antenna module with 360◦ pattern diversity for 5G Internetof- Things,” IEEE Internet Things J., early access, Jul. 28, 2022, doi: 10.1109/JIOT.2022.3194676.

[21] R. Chandel, A. K. Gautam, and K. Rambabu, “Tapered fed compact UWB MIMO-diversity antenna with dual band-notched characteristics,” IEEE Trans. Antennas Propag., vol. 66, no. 4, pp. 1677–1684, Apr. 2018.